

000 MINIMAX LEARNING OF INTERPRETABLE
 001 FACTORED STOCHASTIC POLICIES FROM CONJOINT DATA,
 002 WITH UNCERTAINTY QUANTIFICATION
 003
 004
 005

006 **Anonymous authors**

007 Paper under double-blind review

008 **ABSTRACT**

010 We study offline learning of factored stochastic policies over extremely large,
 011 combinatorial action spaces and show how standard conjoint data can be
 012 used to estimate such policies with valid statistical uncertainty. Conjoint
 013 analyses typically report AMCEs by averaging over opponent attributes
 014 and thus ignore strategic interdependence. We instead learn *stochastic*
 015 *interventions*—product-of-Categorical policies over factor levels—that (i)
 016 optimize expected outcomes in an average-case setting and (ii) extend to
 017 a two-player *minimax* (adversarial) setting that realistically captures si-
 018 multaneous strategic candidate selection. Methodologically, we derive a
 019 closed-form solution for the average-case optimizer under two-way interac-
 020 tions with L_2 variance regularization, and provide a general gradient-based
 021 procedure for richer model classes. Uncertainty from the outcome model
 022 propagates exactly to both the optimal policy and its value via the Delta
 023 method. We further model institutional details (e.g., primaries) inside the
 024 minimax objective and introduce a data-driven measure of strategic diver-
 025 gence between parties. On synthetic data, we characterize sample com-
 026 plexity and coverage as dimensionality and n vary. On a U.S. presidential
 027 conjoint, adversarially learned policies produce equilibrium vote shares that
 028 align with historical election ranges, in stark contrast to non-adversarial
 029 (averaging) optimizers. To facilitate reproducibility and further research,
 030 we release an open-source dataset of mapped historical U.S. presidential
 031 candidate features on Hugging Face. Our framework connects causal pol-
 032 icy learning with multi-agent RL in high-dimensional discrete action spaces
 033 while preserving interpretability and statistical guarantees.

034 Over the past decade, conjoint analysis, which is an application of high-dimensional factorial
 035 design, has become the most popular survey experiment methodology to study multidimen-
 036 sional preferences (Hainmueller et al., 2014). One of the most common political science
 037 applications of conjoint analysis is the evaluation of candidate profiles (e.g., Franchino &
 038 Zucchini, 2015; Ono & Burden, 2019; Christensen et al., 2021; Kirkland & Coppock, 2018).

039 In such experiments, respondents are asked to choose between two hypothetical political
 040 candidates whose features (e.g., gender, race, age, education, partisanship, and policy po-
 041 sitions) are randomly selected. This design often employs a forced-choice format, where
 042 respondents must select one of the two candidates without an option to abstain or express
 043 no preference (Abramson et al., 2023). Researchers then proceed by estimating the average
 044 causal effect of each feature while marginalizing the remaining features over a particular
 045 distribution of choice. This popular quantity of interest is termed the Average Marginal
 046 Component Effect (AMCE) (Hainmueller et al., 2014).

047 AMCEs average a feature’s effect over a chosen distribution for the other features, which
 048 means the answer depends on that averaging choice (de la Cuesta et al., 2019). In practice,
 049 researchers often use a uniform distribution, but real candidate pools are not uniform, and
 050 candidates do not choose their profiles in strategic isolation from opponents.

051 We therefore replace effect estimation with *policy learning*. Instead of asking for the marginal
 052 effect of a single attribute, we learn a *factored stochastic policy* over full profiles: a mixed
 053 distribution that assigns independent categorical probabilities to each attribute level and
 054 thus remains interpretable (one can read off how much weight the policy puts on, say,
 055 “economy” versus “immigration” as policy priority). In the non-adversarial, average-case
 056 setting, this policy is chosen to maximize expected win probability against a fixed reference

054 distribution for the opponent. We control variance and preserve interpretability by shrinking
 055 the learned policy toward the experimental assignment.
 056

057 To capture strategic interaction, we extend to an adversarial setting in which both sides
 058 simultaneously choose their own mixed profile distributions. The objective is minimax—each
 059 side selects a profile distribution that is best against the other’s—and institutional details are
 060 built in. Specifically, we model two stages: primary elections within each party (which induce
 061 a distribution over nominees) followed by the general election. The resulting equilibrium
 062 policies reflect how strategic opponents and institutions jointly shape feasible profile choices.
 063

064 Under a linear outcome model with two-way interactions, the average-case optimizer with
 065 squared-distance regularization has a closed-form solution; uncertainty for both the optimal
 066 policy and its value is obtained by propagating the outcome-model uncertainty using the
 067 Delta method. For richer models, we optimize the logits of the factored policy by gradient
 068 methods while enforcing the simplex constraints implicitly, and we carry uncertainty through
 069 the optimization by differentiating end-to-end. The same machinery applies when we move
 070 from average-case to the adversarial, institution-aware game.
 071

072 **Our contributions are:** (1) A shift from AMCEs to a conjoint estimand that is a factored
 073 stochastic policy over profiles, learned to maximize expected electoral performance, and in-
 074 terpretable at the attribute-level. (2) A closed-form average-case optimizer under two-way
 075 interactions with squared-distance variance control, together with uncertainty quantification
 076 for both the optimal policy and its value via the Delta method. (3) A general gradient-based
 077 procedure for richer outcome models (including regularized GLMs and neural models) with
 078 end-to-end differentiation for standard errors. (4) An adversarial, minimax extension that
 079 embeds institutional structure (primaries then general), yielding equilibrium mixed strate-
 080 gies and a data-driven measure of strategic divergence between parties. (5) Empirical evi-
 081 dence from simulations and a U.S. presidential conjoint showing that adversarially learned
 082 policies produce equilibrium vote shares aligned with historical ranges, plus an open-source
 083 mapping of historical candidate features to conjoint levels to facilitate replication.
 084

085 **Related literature.** We contribute to the methodological literature on conjoint analysis
 086 and policy learning. In the growing field of conjoint analysis, we are, to our knowledge, the
 087 first to address optimal profile selection, particularly in adversarial settings. Related work
 088 in sequential decision-making includes multi-armed bandit problems (Audibert et al., 2010),
 089 while non-sequential conjoint studies focus on causal effect estimation (Hainmueller et al.,
 090 2014; Egami & Imai, 2019; de la Cuesta et al., 2019), hypothesis testing (Ham et al., 2022;
 091 Liu & Shiraito, 2023), causal estimand interpretation (Abramson et al., 2022), experimental
 092 design (Bansak et al., 2018), and stable preference analysis (Abramson et al., 2022; 2023).
 093 We also connect to causal inference literature on treatment rules, where recent advances in
 094 policy learning from granular data—both experimental and observational—have proliferated
 095 (see e.g., Dudik et al., 2011; Imai & Strauss, 2011; Zhao et al., 2012; Kitagawa & Tetenov,
 096 2018; Athey & Wager, 2021; Ben-Michael et al., 2021; Kallus & Zhou, 2021; Zhang et al.,
 097 2022, and others), yielding individualized rules for binary treatments based on observables.
 098

099 Our work can be seen as framing our problem as an offline contextual bandit with combi-
 100 natorial actions, where conjoint randomization serves as the logging policy. The proposed
 101 optimal stochastic intervention learns a mixed policy over candidate attributes—a factor-
 102 ized Categorical distribution for interpretability and variance control—extending welfare-
 103 oriented policy learning (Kitagawa & Tetenov, 2018; Athey & Wager, 2021). The adversarial
 104 case models a two-player zero-sum game, with equilibria as minimax solutions to a single-step
 105 Markov game (Littman, 1994). Conjoint randomization identifies counterfactuals via direct
 106 modeling or off-policy estimators (e.g., doubly robust (Dudik et al., 2011)), sidestepping off-
 107 line RL confounding (Levine et al., 2020). Overall, we adapt these tools to high-dimensional
 108 conjoints for interpretable stochastic policies and equilibria with uncertainty quantification.
 109

110 LEARNING FACTORED STOCHASTIC POLICIES FROM CONJOINT DATA

111 Suppose that we have a simple random sample of n respondents from a population. We
 112 consider a conjoint design of candidate choice with a total of D factorial features per can-
 113 didate. Each factorial feature $d \in \{1, 2, \dots, D\}$ has $L_d \geq 2$ levels. The random variable
 114 representing an entire candidate profile presented to respondent i in the design is labeled

108 \mathbf{T}_i . The support of \mathbf{T}_i , denoted \mathcal{T} , is the space of all possible treatment assignments and
 109 will vary based on the experimental design. For example, if each feature has L levels, i.e.,
 110 $L_1 = \dots = L_D = L$, we have $\mathbf{t} \in \mathcal{T} = \{1, 2, \dots, L\}^D$, where \mathbf{t} is a specific realization of \mathbf{T}_i .

111 Usually, each respondent i faces a choice between two candidate profiles, \mathbf{T}_i^a and \mathbf{T}_i^b . The
 112 observed outcome will be an indicator of whether candidate a is chosen over b , which occurs
 113 when the latent utility of a , represented as $Y_i(\mathbf{T}_i^a)$, is higher than that of b , which is repre-
 114 sented as $Y_i(\mathbf{T}_i^b)$. This choice variable can be quantified as $C(\mathbf{T}_i^a, \mathbf{T}_i^b) = \mathbb{I}\{Y_i(\mathbf{T}_i^a) > Y_i(\mathbf{T}_i^b)\}$,
 115 representing the standard paired-profile conjoint in which respondents must select exactly
 116 one of two profiles as preferable, so that $C(\mathbf{T}_i^a, \mathbf{T}_i^b) \in \{0, 1\}$ (Hainmueller et al., 2014).

117 Often, each treatment combination is equally likely to be realized, in which case
 118 $\Pr(\mathbf{T}_i = \mathbf{t}) = |\mathcal{T}|^{-1}$ for all treatment combinations, \mathbf{t} . When factor levels have possibly
 119 different assignment probabilities, some treatment combinations will be more likely than
 120 others. Usually, each factor is assigned using draws from independent Categorical distribu-
 121 tions so that we can write the probability of treatment combination \mathbf{t} as

$$123 \quad \Pr(\mathbf{T}_i = \mathbf{t}) = \prod_{d=1}^D \prod_{l=1}^{L_d} p_{dl}^{\mathbb{I}\{t_d = l\}},$$

124 where p_{dl} is the Categorical probability for factor d taking on level l and $\mathbb{I}\{t_d = l\}$ is the
 125 indicator function that is 1 when t_d takes on value l and 0 otherwise. We let \mathbf{p} define the
 126 vector of Categorical probabilities defining the data-generating distribution.

127 For simplicity, we make standard assumptions of conjoint analysis. That is, we assume that
 128 there is no interference between units and that the treatment assignment is randomized,
 129 i.e., $\{Y_i(\mathbf{t}^a), Y_i(\mathbf{t}^b)\} \{ \mathbf{T}_i^a, \mathbf{T}_i^b \}$ and $\Pr(\mathbf{T}_i^c = \mathbf{t}^c) > 0$ for $c \in \{a, b\}$ and all $\mathbf{t}^c \in \mathcal{T}$.

130 **Optimal Selection of Conjoint Profiles in a Non-Adversarial Setting.** We consider
 131 the optimal selection of conjoint profiles, enabling us to study the types of political candi-
 132 dates who are likely to receive greater support from different types of voters. The standard
 133 approach, dominant in the policy learning literature, is to identify the following optimal
 134 treatment combination, $\mathbf{t}^* = \arg \max_{\mathbf{t} \in \mathcal{T}} \mathbb{E}[Y_i(\mathbf{t})]$, where \mathbf{t}^* is the treatment combination
 135 that maximizes the average value of some generic outcome, Y_i . In the forced-choice conjoint
 136 case, this quantity would amount to $\mathbf{t}^{a*} = \arg \max_{\mathbf{t}^a \in \mathcal{T}} \mathbb{E}[C(Y_i(\mathbf{t}^a), Y_i(\mathbf{T}_i^b))]$, so investigators
 137 find the vote-share-maximizing candidate profile \mathbf{t}^{a*} , averaging over opposing candidate b
 138 features (as in AMCE analysis). This approach has two limitations. First, high-dimensional
 139 treatments in conjoint analysis prevent identifying \mathbf{t}^* , as $|\mathcal{T}|$ far exceeds the sample size.
 140 Second, when multiple equally optimal profiles exist, identifying several is more informative
 141 than a single one.

142 To address this challenge, we propose finding an optimal stochastic intervention: we con-
 143 sider a parametric distribution of profiles $\Pr_{\boldsymbol{\pi}}(\cdot)$ that maximizes the average outcome. By
 144 considering a parametric model, we are able to effectively summarize a set of profiles that
 145 perform well. Formally, we seek the optimal stochastic intervention,

$$146 \quad Q(\boldsymbol{\pi}^*) = \max_{\boldsymbol{\pi}} Q(\boldsymbol{\pi}) \quad \text{where} \quad Q(\boldsymbol{\pi}) = \sum_{\mathbf{t} \in \mathcal{T}} \mathbb{E}[Y_i(\mathbf{t})] \Pr_{\boldsymbol{\pi}}(\mathbf{T}_i = \mathbf{t}), \quad (1)$$

147 where $\boldsymbol{\pi}$ parameterizes the distribution of profiles. In the forced-choice conjoint case, this
 148 quantity can be written in the average case as agent A optimizing their strategy, averaging
 149 over B 's fixed strategy:

$$150 \quad Q(\boldsymbol{\pi}^{a*}) = \max_{\boldsymbol{\pi}^a} \sum_{\mathbf{t}^a, \mathbf{t}^b \in \mathcal{T}} \mathbb{E}\left[C(Y_i(\mathbf{T}_i^a), Y_i(\mathbf{T}_i^b))\right] \Pr_{\boldsymbol{\pi}^a}(\mathbf{T}_i^a = \mathbf{t}^a) \Pr_{\mathbf{p}}(\mathbf{T}_i^b = \mathbf{t}^b).$$

151 The interpretation here is that $\boldsymbol{\pi}^{a*}$ characterizes the highest possible vote share for a given
 152 counterfactual strategy of assigning the candidate characteristics of a , while features of b
 153 are assigned according to a static averaging distribution (e.g., uniform).

154 Building on Equation 1, we preserve interpretability by restricting the counterfactual pro-
 155 file distribution for candidate a to the same product-of-Categoricals used by the
 156 conjoint randomization $\Pr_{\mathbf{p}}$. Concretely, $\Pr_{\boldsymbol{\pi}^a}(\mathbf{T}_i^a = \mathbf{t}^a)$ has the identical factorized form

162 as $\Pr_{\mathbf{p}}(\mathbf{T}_i = \mathbf{t})$, but with per-attribute probabilities $\boldsymbol{\pi}^a$ replacing \mathbf{p} . This choice yields
 163 an attribute-readable policy and keeps off-policy evaluation tractable. The deterministic
 164 “best profile” appears as a degenerate special case, $\Pr_{\boldsymbol{\pi}^*}(\mathbf{T}_i = \mathbf{t}) = \mathbb{I}(\mathbf{t} = \mathbf{t}^*)$, but in high-
 165 dimensional conjoints that target is unidentifiable and statistically brittle; we therefore
 166 optimize over *stochastic* policies that summarize families of high-performing profiles.

167 To allow meaningful deviations from the design while controlling variance, we impose an L_2
 168 (or KL) trust-region around the logging distribution:
 169

$$170 \max_{\boldsymbol{\pi}^a} Q(\boldsymbol{\pi}^a) - \lambda_n \|\boldsymbol{\pi}^a - \mathbf{p}\|_2^2,$$

172 equivalently constraining $\|\boldsymbol{\pi}^a - \mathbf{p}\|_2 \leq \epsilon_n$. This regularization is motivated by the increase
 173 in off-policy variance as $\boldsymbol{\pi}^a$ departs from \mathbf{p} . The restriction-regularization pair—matching
 174 the conjoint’s factorized assignment and shrinking toward \mathbf{p} —is important because it (i)
 175 preserves interpretability, (ii) stabilizes estimation, and (iii) yields a closed-form average-
 176 case optimizer under two-way interactions (Proposition 1), while still admitting general
 177 gradient-based solutions for richer (e.g., neural) outcome models.

178 **Outcome model (Bernoulli GLM).** Let $C_i = \mathbb{I}\{Y_i(\mathbf{T}_i^a) > Y_i(\mathbf{T}_i^b)\}$ denote the forced
 179 choice. We model $C_i \mid (\mathbf{T}_i^a, \mathbf{T}_i^b) \sim \text{Bernoulli}(\sigma(\eta_i))$, where $\sigma(x) = \{1 + \exp(-x)\}^{-1}$ is the
 180 logistic link and

$$181 \eta_i = \tilde{\mu} + \sum_{d=1}^D \sum_{l=1}^{L_d} \beta_{dl} (\mathbb{I}\{T_{id}^a = l\} - \mathbb{I}\{T_{id}^b = l\}) + \sum_{d < d'} \sum_{l=1}^{L_d} \sum_{l'=1}^{L_{d'}} \gamma_{dl,d'l'} (\mathbb{I}\{T_{id}^a = l, T_{id'}^a = l'\} - \mathbb{I}\{T_{id}^b = l, T_{id'}^b = l'\}).$$

184 where β_{dl} denotes the main effect of factor d with level l , $\gamma_{dl,d'l'}$ denotes the interaction
 185 effect of treatment $d'l'$ and $d'l''$. We impose sum-to-0 constraints on $\{\beta_{dl}\}_l$ and on each
 186 $\{\gamma_{dl,d'l'}\}_{l,l'}$ for identifiability (Egami & Imai, 2019). Parameters $(\tilde{\mu}, \boldsymbol{\beta}, \boldsymbol{\gamma})$ are estimated via
 187 GLM (e.g., logistic) with optional sparsity (lasso) if desired. An intuition here is that the
 188 difference between utilities under candidates a and b defines the choice between a and b .
 189

190 This model makes calculation of the average outcome under a stochastic intervention
 191 straightforward if the policies, $\boldsymbol{\pi}^a$ and $\boldsymbol{\pi}^b$, over candidate a and b features define Cate-
 192 gorical distributions. Then, the *Stochastic Intervention Under Forced Choice Conjoint* can
 193 be written as:

$$194 Q(\boldsymbol{\pi}^a, \boldsymbol{\pi}^b) = \mathbb{E}_{\mathbf{T}^a \sim \boldsymbol{\pi}^a, \mathbf{T}^b \sim \boldsymbol{\pi}^b} \left[\sigma \left(\tilde{\mu} + \sum_{d,l} \beta_{dl} (\mathbb{I}\{T_d^a = l\} - \mathbb{I}\{T_d^b = l\}) + \sum_{d < d'} \sum_{l,l'} \gamma_{dl,d'l'} (\mathbb{I}\{T_d^a = l, T_{d'}^a = l'\} - \mathbb{I}\{T_d^b = l, T_{d'}^b = l'\}) \right) \right].$$

195 Under a linear probability approximation, this becomes:

$$196 Q(\boldsymbol{\pi}^a, \boldsymbol{\pi}^b) = \mathbb{E}_{\boldsymbol{\pi}^a, \boldsymbol{\pi}^b} \left[\Pr(Y_i(\mathbf{T}_i^a) > Y_i(\mathbf{T}_i^b)) \right] = \tilde{\mu} + \sum_{d=1}^D \sum_{l=1}^{L_d} \beta_{dl} (\pi_{dl}^a - \pi_{dl}^b) + \sum_{d,d':d < d'} \sum_{l=1}^{L_d} \sum_{l'=1}^{L_{d'}} \gamma_{dl,d'l'} (\pi_{dl}^a \pi_{dl'}^a - \pi_{dl}^b \pi_{dl'}^b).$$

201 Motivated by the opponent candidate marginalization in AMCE analysis, we first consider
 202 the optimal average-case stochastic intervention where a optimizes against a uniform dis-
 203 tribution over candidate features. In this case, $\boldsymbol{\pi}^{a*}$, can here be derived in closed form,
 204 assuming the features of the opposing candidate, b , are assigned according to a fixed dis-
 205 tribution such as \mathbf{p} . We will call this kind of analysis the *Average Case Optimal Stochastic*
 206 *Intervention for Forced-Choice Conjoint* in that the behavior of the opponent, b , is static.
 207

208 **PROPOSITION 1** *Under a linear-probability approximation and with two-way interactions
 209 and L_d levels for factor d , the average-case optimal L_2 regularized stochastic intervention
 210 is, for large enough value of λ_n , given by*

$$211 \boldsymbol{\pi}^{a*} = \mathbf{C}^{-1} \mathbf{B}, \text{ where } B_{r(dl),1} = -\beta_{dl} - 4\lambda_n p_{dl} - 2\lambda_n \sum_{l' \neq l, l' < L_d} p_{dl'} \\ 212 C_{r(dl),r(dl)} = -4\lambda_n; C_{r(dl),r(dl')} = -2\lambda_n; C_{r(dl),r(d'l'')} = \gamma_{dl,d'l''},$$

213 where $r(dl)$ denotes an indexing function returning the position associated with its factor d
 214 and level l into the rows of B and rows or columns of C . For proof, see §A.I.2.

216 Here, the optimal stochastic intervention, $\Pr_{\pi^{a^*}}$, is a deterministic function of the outcome
 217 model parameters. The parameters defining the outcome model, β and γ , are not known *a*
 218 *priori*, but can be estimated via GLM, with uncertainties calculated using asymptotic SEs.
 219

220 Intuitively, the analysis done here allows researchers to investigate the implications of models
 221 for candidate choice fit on the data. Instead of examining marginals via AMCE, they can
 222 examine joint effects by looking at the optimal behavior implied under their choice of model.
 223 Estimates of the optimal distribution over candidates are generated using uncertain model
 224 parameters; however, the Delta method enables the rigorous propagation of uncertainty.
 225

226 Because the values, π^{a^*} defining $\Pr_{\pi^{a^*}}$ are a deterministic function of modeling parameters,
 227 the variance-covariance matrix of $\{\hat{Q}(\hat{\pi}^{a^*}), \hat{\pi}^{a^*}\}$ can be obtained via the Delta method:
 228

$$\text{Var-Cov}(\{\hat{Q}(\hat{\pi}^{a^*}), \hat{\pi}^{a^*}\}) = \mathbf{J} \hat{\Sigma} \mathbf{J}',$$

229 where $\hat{\Sigma}$ is the variance-covariance matrix from the modeling strategy for Y_i using regression
 230 parameters $\{\beta, \gamma\}$ and \mathbf{J} is the Jacobian of partial derivatives (e.g., of $\hat{Q}(\hat{\pi}^{a^*})$ and $\hat{\pi}^{a^*}$
 231 w.r.t. the outcome model parameters): $\mathbf{J} = \nabla_{\{\beta, \gamma\}} \{\hat{Q}(\hat{\pi}^{a^*}), \hat{\pi}^{a^*}\}$. Under i.i.d., correct
 232 specification, regularity conditions, and standard moment conditions of the MLE,
 233

$$\sqrt{n} \left(\{\hat{Q}(\hat{\pi}^{a^*}), \hat{\pi}^{a^*}\} - \{Q(\pi^{a^*}), \pi^{a^*}\} \right) \rightarrow \mathcal{N}(\mathbf{0}, \mathbf{J} \Sigma \mathbf{J}').$$

234 The approach here thereby gives researchers a recipe for finding optimal stochastic interventions
 235 given choice of outcome model. Uncertainties from the outcome model parameters
 236 propagate into uncertainties over the optimal strategy. In sum, a closed-form expression
 237 for the regularized optimal stochastic intervention can be found in the base case of conjoint
 238 analysis where one candidate optimizes against a fixed opponent distribution.
 239

240 **General Optimal Stochastic Interventions in Non-Adversarial Environments.** There are limitations to the approach just described. One limitation is that while preserving the sum-to-1 constraint on the probabilities, the analytical solution in Proposition 1 does not guarantee the non-negativity of $\hat{\pi}^{a^*}$ for small values of λ_n . Another limitation is that, as soon as we generalize the outcome model to the GLM or > 2 -way interactions, we have no analytical formula for the optimal solution.
 241

242 To address these limitations, we can perform the stochastic intervention optimization for
 243 $\hat{\pi}^{a^*}$ using iterative methods instead of an analytical closed form.¹ For example, to ensure
 244 that the entries in $\hat{\pi}^{a^*}$ lie on the simplex, we can re-parameterize the objective function
 245 using α_{dl} 's, which inhabit an unconstrained space (see §A.I.7) for details). In particular,
 246 the stochastic interventional factor probabilities, π , are now a function of a , defined as so:
 247

$$\Pr_{\pi(a)}(T_d = l) = \begin{cases} \frac{\exp(\alpha_{dl})}{1 + \sum_{l'=1}^{L_d-1} \exp(\alpha_{dl'})} & \text{if } l < L_d \\ \frac{1}{1 + \sum_{l'=1}^{L_d-1} \exp(\alpha_{dl'})} & \text{if } l = L_d \text{ (baseline category)} \end{cases}$$

248 We can optimize this via gradient ascent, which, for almost every starting point, arrives at
 249 least at a local maximum or stationary point in polynomial time, assuming the strict saddle
 250 property of the function to be optimized (Lee et al., 2016). We update the unconstrained
 251 parameters using the gradient information, $\nabla_{\alpha} \{O(a)\}$, where the full expression is found in
 252 §A.I.4. In particular, we iteratively update the initial state of a in S gradient ascent update
 253 steps:
 254

$$\underbrace{\{\text{for } s \in \{1, \dots, S\} : \{\alpha^{(s+1)} := \alpha^{(s)} + \gamma^{(s)} \nabla_{\alpha} \{O(\alpha^{(s)})\}\}\}}_{\text{gradients traced through all } S \text{ updates for Jacobian } \mathbf{J}}$$

255 Inference proceeds analogously to the closed-form case, via the delta method. With a closed-
 256 form expression for $\hat{\pi}^{a^*}$, it is evident how we could write an expression for the derivative of
 257 optimal as a function of the regression parameters using the closed-form Jacobian. With an
 258

259 ¹With two-way interactions, this setup can be framed as a quadratic programming problem with
 260 linear constraints, which can be solved efficiently using interior point or simplex methods. We focus
 261 on gradient ascent as a more general solution, allowing neural network models of outcome.

270 iterative computation needed to obtain $\hat{\pi}^{a^*}$, we can consider the same quantity: although the
 271 closed-form derivatives of the iterative solution may be unknown, we can still evaluate these
 272 values using automatic differentiation—tracing the gradient information through the entire
 273 sequence of S gradient ascent updates. Specifically, since the ascent procedure defines a
 274 deterministic mapping from $\hat{\beta}, \hat{\gamma}$ to $\hat{\pi}^{a^*}$ (and thence to $\hat{Q}(\hat{\pi}^{a^*})$), reverse-mode differentiation
 275 can backpropagate sensitivities through the full unrolled sequence of S updates, yielding \mathbf{J} .

276 **Adversarial Dynamics.** Thus far, we have considered optimal stochastic interventions
 277 under the assumption that one party (or candidate) chooses its profile distribution to maxi-
 278 mize expected vote share, while treating the distribution of the opposing candidate’s profile
 279 as fixed. Although this framework is useful in settings without direct strategic interaction
 280 (e.g., analyzing hiring choices), it is less suitable when two agents strategically select their
 281 own profiles in direct electoral competition. In many contexts, both the focal candidate and
 282 the opposing candidate are engaged in simultaneous strategic optimization.

283 To capture these adversarial dynamics, we introduce an *Adversarial Case Optimal Stochastic*
 284 *Intervention* framework that explicitly models two agents, which we label as A and B , each
 285 attempting to maximize their expected probability of victory in a forced-choice setting. This
 286 is a two-player, simultaneous action zero-sum game. Let $Y_i(\mathbf{T}_i^c)$ represent respondent i ’s
 287 latent utility for candidate $c \in \{A, B\}$, where \mathbf{T}_i^c is the candidate’s profile randomly drawn
 288 from some distribution. The observed forced-choice outcome is:

$$289 \quad 290 \quad C(\mathbf{T}_i^A, \mathbf{T}_i^B) = \mathbb{I}\{Y_i(\mathbf{T}_i^A) > Y_i(\mathbf{T}_i^B)\}.$$

291 We define candidate profile distributions for A and B as π^A and π^B , respectively. Each dis-
 292 tribution assigns probabilities to the set of all possible profiles, \mathcal{T} . The choice of a stochastic
 293 (mixed) rather than deterministic profile stems from the combinatorics of potential profiles
 294 and impossibility of identifying a unique optimal profile with finite samples.

295 We consider a *zero-sum* environment where one candidate’s gain is the other’s loss. In
 296 this setting, it is natural to characterize the optimal profile distributions through a min-
 297 max optimization problem. Letting $Q(\pi^A, \pi^B) = \mathbb{E}_{\pi^A, \pi^B}[C(\mathbf{T}_i^A, \mathbf{T}_i^B)]$ denote the expected
 298 probability that candidate A wins against candidate B , the adversarial objective is:

$$299 \quad 300 \quad \max_{\pi^A} \min_{\pi^B} Q(\pi^A, \pi^B). \quad (3)$$

301 In equilibrium, neither candidate can improve their expected performance by unilaterally
 302 changing their distribution. Such a pair (π^{A^*}, π^{B^*}) constitutes a Nash equilibrium for the
 303 adversarial environment, evoking classic results in game theory (Kreps, 1989). In other
 304 words, given π^{B^*} , no deviation from π^{A^*} improves A ’s performance, and vice versa.

306 **Institutional Constraints.** Without institutional asymmetries, the adversarial game just
 307 described can admit trivial or symmetric equilibria. Real strategic environments such as
 308 elections, however, are structured by rules that determine *who* votes *when*, and therefore
 309 shape both feasible strategies and equilibria. We model a two-stage system—party primaries
 310 followed by a general election—under potentially asymmetric institutions across parties.

311 Let A and B index the two parties. Denote by \mathcal{I}^A and \mathcal{I}^B the (possibly overlapping) primary
 312 electorates for A and B , respectively (closed, semi-open, and open primaries are special
 313 cases), and by \mathcal{E} the general-election electorate. Institutions determine these sets and their
 314 sampling weights (e.g., turnout, inclusion of independents); we bundle these parameters as \beth .
 315 Each party $c \in \{A, B\}$ chooses a factored, product-of-Categorical mixed profile distribution
 316 π^c (our policy); the rest of that party’s field is summarized by a counter-distribution $\pi^{c'}$.²

317 **Primary Stage (Pairwise Head-to-head Model).** For two profiles $\mathbf{t}, \mathbf{t}' \in \mathcal{T}$ and party
 318 c , define the primary head-to-head win probability

$$319 \quad 320 \quad \kappa_c(\mathbf{t}, \mathbf{t}') = \mathbb{E}_{i \in \mathcal{I}^c}[C(\mathbf{t}, \mathbf{t}')] = \Pr_{i \in \mathcal{I}^c}(Y_i(\mathbf{t}) > Y_i(\mathbf{t}')),$$

322 ²Empirically, $\pi^{c'}$ can be an empirical mixture over other entrants, a calibrated baseline, or
 323 set equal to π^c under symmetry. Multi-candidate or multi-round procedures can be handled by
 replacing the pairwise mechanism below with the appropriate implied choice probabilities.

324 where $C(\cdot, \cdot)$ is the forced-choice indicator introduced earlier. In a large electorate, $\kappa_c(t, t')$
 325 approximates the majority outcome. A simple and differentiable pushforward from *primary*
 326 *strategies* to the *nominee distribution* is obtained by drawing one entrant from the party
 327 strategy and one from the field (drawn from the counter distribution, $\pi^{c'}$):
 328

$$\pi^c(t) = \underbrace{\pi^c(t) \mathbb{E}_{t' \sim \pi^{c'}} [\kappa_c(t, t')]}_{t \text{ drawn as party entrant and wins}} + \underbrace{\pi^{c'}(t) \mathbb{E}_{t' \sim \pi^c} [1 - \kappa_c(t', t)]}_{t \text{ drawn from field and defeats the party entrant}}. \quad (4)$$

330 Thus $\bar{\pi}^c$ is the induced distribution over the party’s nominee after the primary.
 331

333 **Independence Across Primaries.** Conditional on profiles and voter utilities, we assume
 334 the two primaries resolve independently,
 335

$$\left\{ \mathbb{I}[Y_i(t) > Y_i(t')] \right\}_{i \in \mathcal{I}^A} \perp \left\{ \mathbb{I}[Y_j(u) > Y_j(u')] \right\}_{j \in \mathcal{I}^B} \mid t, t', u, u', \square \quad (5)$$

336 which permits factorization of the joint nominee distribution as $\bar{\pi}^A \otimes \bar{\pi}^B$.
 337

339 **General Election and Institutionalized Value.** Given nominees $t \sim \bar{\pi}^A$ and $u \sim \bar{\pi}^B$,
 340 the probability that A wins the general election—averaging over the general electorate \mathcal{E} —is
 341 $\mathbb{E}_{i \in \mathcal{E}} [C(t, u)] = \Pr_{i \in \mathcal{E}} (Y_i(t) > Y_i(u))$. The expected (institution-aware) payoff to A is then
 342

$$Q_{\text{inst}}(\pi^A, \pi^B; \pi^{A'}, \pi^{B'}, \square) = \mathbb{E}_{\substack{t \sim \bar{\pi}^A(\pi^A, \pi^{A'}, \square) \\ u \sim \bar{\pi}^B(\pi^B, \pi^{B'}, \square)}} \left[\mathbb{E}_{i \in \mathcal{E}} [C(t, u)] \right]. \quad (6)$$

346 **Equilibria Under Institutions.** The minimax problem over interpretable, variance-
 347 controlled policies using factored, product-of-Categorical distributions, $\Pi_{\text{fact}}^A, \Pi_{\text{fact}}^B \subset \Delta(\mathcal{T})$
 348 becomes (assuming fixed $\pi^{A'}, \pi^{B'}$):
 349

$$\max_{\pi^A} \min_{\pi^B} Q_{\text{inst}}(\pi^A, \pi^B; \pi^{A'}, \pi^{B'}, \square),$$

351 defining a *restricted minimax* problem. Von Neumann’s minimax theorem guarantees a
 352 saddle point on the full simplices $\Delta(\mathcal{T}) \times \Delta(\mathcal{T})$; however, within the restricted factored
 353 distribution class, Π_{fact}^c is in general non-convex, so a saddle point need not exist within the
 354 restricted class. In practice, we compute a stationary point via gradient ascent–descent on
 355 unconstrained logits; see Appendix for a discussion of how to certify how close the learned
 356 pair $(\hat{\pi}^A, \hat{\pi}^B)$ is to a full mixed-strategy equilibrium.
 357

We evaluate the pushforward map $\pi^c \mapsto \bar{\pi}^c$ by re-parameterized Monte Carlo over $t \sim \pi^c$
 358 and $t' \sim \pi^{c'}$ and optimize via gradient-based ascent–descent on the unconstrained logits
 359 that parameterize the factored Categorical policies, with KL or L_2 variance-control regu-
 360 larization from Eq. 1. As in the non-institutional case, Delta-method inference follows by
 361 backpropagating sensitivities of Q_{inst} to the outcome-model parameters through the unrolled
 362 optimization, yielding standard errors for $\hat{\pi}^A, \hat{\pi}^B$ and \hat{Q}_{inst} .
 363

364 **Remarks.** (i) Open vs. closed primaries, heterogeneous turnouts, and the participation
 365 of independents are encoded by \square via the composition/weighting of \mathcal{I}^A , \mathcal{I}^B , and \mathcal{E} . (ii)
 366 Hard rules (eligibility constraints, ballot-access requirements) are enforced by restricting the
 367 support of π^A and π^B to admissible profiles. (iii) Multi-round or multi-candidate primaries
 368 can be accommodated by replacing κ_c with the appropriate implied choice probabilities; the
 369 pushforward Eq. 4 remains a differentiable functional of $(\pi^c, \pi^{c'}, \square)$. The framework here
 370 can accommodate respondent covariates; see Appendix.

371 **Quantifying Strategic Divergence.** Unlike AMCE analysis, which cannot quantify ob-
 372 served candidate information through experimental findings, the methodology here enables
 373 the measurement of strategic divergence using actual candidate profiles and the elicited
 374 conjoint preferences. In particular, given the optimal candidate distribution for one party,
 375 π^A , and another, π^B , in a given institutional context, we can find the strategic divergence
 376 factor, \mathcal{D} , of a given candidate profile, t , using the estimated strategies:
 377

$$\mathcal{D}(t) = \left| \log \left(\frac{\Pr_{\pi^A}(t)}{\Pr_{\pi^B}(t)} \right) \right| = \left| \log \{ \Pr_{\pi^A}(t) \} - \log \{ \Pr_{\pi^B}(t) \} \right|. \quad (7)$$

378 When $\mathcal{D}(\mathbf{t})$ is 0, the candidate profile \mathbf{t} would be equally likely under the strategic action
 379 of party A and B ; when $\mathcal{D}(\mathbf{t})$ is large, this is an indication that a given profile would be
 380 likely under the strategy of one party, but unlikely under the strategy of another.

381 EXPERIMENTS: SYNTHETIC SCALING & SAMPLE COMPLEXITY

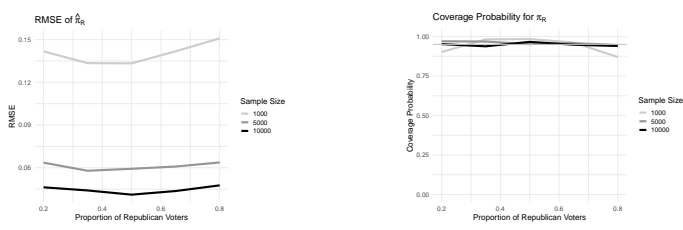
383 **Average Case Simulation.** In Monte Carlo simulations using synthetic binary conjoint
 384 data under a linear outcome model with interactions (scaled to $R^2 = 0.70$ for main effects),
 385 we assess finite-sample convergence of the average-case optimal stochastic intervention by
 386 varying sample sizes ($n \in 500, 1500, 3500, 10000$) and dimensions ($K \in 5, 10, 20$), with L_2
 387 regularization tuned to diverge moderately from the uniform data-generating distribution.
 388 Results demonstrate negligible bias and rapidly declining RMSE (variance-dominated) for
 389 $\hat{\pi}^*$ and $\hat{Q}(\hat{\pi}^*)$ even at small n , with inference reliable as coverage nears nominal levels across
 390 settings; details, including Figures 4–9, are in §A.I.8. This approach also substantially
 391 outperforms a baseline AMCE-based policy (selecting per-factor maximizers), achieving
 392 higher expected outcomes on average; see Figure 5 and Appendix for details.

393 **Adversarial Case Simulation Design.** To assess finite-sample performance in the ad-
 394 versarial setting, we simulate two-party strategic competition between Republicans (R) and
 395 Democrats (D) in a two-stage electoral process: primaries for nominee selection, followed by
 396 a general election. Voters are affiliated with R (fraction p_R) or D ($p_D = 1 - p_R$), with only
 397 affiliated voters participating in their primary. We grid over $p_R \in \{0.2, 0.3, 0.5, 0.65, 0.8\}$
 398 and sample sizes $n \in \{1000, 5000, 10000\}$, with Monte Carlo replications per cell.

399 In primaries, each party offers two profiles ($\mathbf{T}_i^{R,1}, \mathbf{T}_i^{R,2}$ for R ; similarly for D), with one
 400 selected via the party’s mechanism and the other uniform. Voter choices follow logistic
 401 models based on features (gender, for tractable ground-truth equilibria). General elections
 402 pit primary winners ($\mathbf{T}_i^{R,*}, \mathbf{T}_i^{D,*}$) against each other, with all voters choosing via separate
 403 R - and D -specific logistic models.

404 Ground-truth mixed strategies π^R, π^D approximate Nash equilibria via grid search, max-
 405 imizing $Q(\pi^R, \pi^D) = \mathbb{E}[\Pr(Y_i(\mathbf{T}_i^R) > Y_i(\mathbf{T}_i^D))]$. Equilibria satisfy $\max_{\pi^R} \min_{\pi^D} Q = \min_{\pi^D} \max_{\pi^R} Q$, where neither party can unilaterally improve expected vote share. For
 406 each run, we estimate equilibria and outcomes, evaluating how p_R and n affect strategies
 407 and vote shares. We report RMSE and 95% CI coverage for π^R . (Details in §A.4.)

409 **Adversarial Case Simulation Results.** Simulation results indicate that the estimation
 410 error depends primarily on the conjoint sample size, with only modest sensitivity to the
 411 proportion of Republican voters. Larger sample sizes reduce uncertainty by stabilizing the
 412 estimates of voter utilities: with larger sample sizes, the overall estimation error declines
 413 sharply for all values of p_R . Coverage rates fall below the nominal level for $n = 1000$ but
 414 approach the nominal 95% level for larger sample sizes. The stronger performance under
 415 increasing n reflects the fact that voters’ utilities are more precisely estimated, allowing
 416 us to obtain better approximations of the zero-sum equilibrium in a two-party adversarial
 417 competition. In sum, these simulations highlight the key role of sample size and voter-party
 418 composition in estimating equilibrium strategies under adversarial conditions. Next, we
 419 apply these approaches to real data to explore optimal strategic dynamics in practice.



420
 421 **Figure 1:** Finite-sample performance of $\hat{\pi}^R$ in the adversarial simulation. The top panel shows the root-
 422 mean-squared error (RMSE) of $\hat{\pi}^R$ for different sample sizes and proportions of Republican voters, p_R . The
 423 bottom panel illustrates the coverage probability of 95% confidence intervals for components of $\hat{\pi}^R$.
 424
 425
 426
 427
 428

429 EXPERIMENTS: REAL-WORLD CONJOINT (U.S. PRESIDENTIAL)

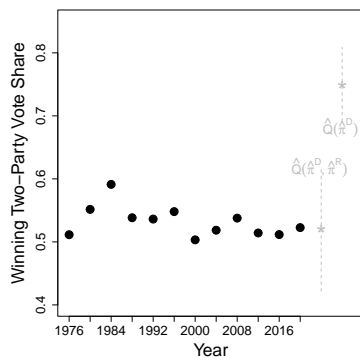
430 We now apply our methods to analyze policy positioning and optimal candidate selection
 431 using presidential preference data from Ono & Burden (2019). Here, our outcome is a

432 binary indicator stating whether candidate a or b was selected by respondent i in a forced
 433 conjoint experiment. In the latent utility formulation above, this can be characterized as
 434 $C(Y_i(\mathbf{T}_i^a), Y_i(\mathbf{T}_i^b))$ —an indicator indicating whether profile \mathbf{T}_i^a yields higher utility for the
 435 respondent than profile \mathbf{T}_i^b ; see §A.1 for a list of candidate factors. (Here, all standard
 436 errors for Delta method uncertainty propagation are clustered at the respondent level.)
 437

438 **Average vs. Adversarial Case Results.** We optimize expected vote share for subpopula-
 439 tions (all, Democrats, Republicans, independents) against a uniform opponent distribution,
 440 using a GLM with interactions (lasso-regularized coefficients). Optimal stochastic inter-
 441 ventions (Fig. 6) diverge on immigration, abortion, and policy expertise (e.g., economy
 442 vs. public safety preferences), but converge on personality traits. Under closed primaries,
 443 we compute minimax equilibria for Republican vs. Democrat strategies. Optimal policies
 444 (Fig. 7) differ from average-case (Fig. A.III.2); e.g., Democrats deprioritize immigration in
 445 average case but counter Republican guest-worker stances adversarially. Equilibrium vote
 446 shares drop markedly (Fig. A.III.1), aligning closer to historical elections.

447 **Results with Data-Driven Clustering.** Prior analyses of regularized optimal stochastic
 448 interventions—with and without adversarial dynamics—ignored respondent characteristics
 449 beyond party affiliation. Yet, heterogeneous voter types often favor distinct candidate pro-
 450 files. To uncover these differences, we apply optimal stochastic interventions under data-
 451 driven respondent clustering, revealing how subgroups respond uniquely to high-dimensional
 452 features. Leveraging the clustered outcome model of Goplerud et al. (2022), Fig. 11 shows
 453 that covariate-sensitive strategies recover the underlying Democrat-Independent-Republican
 454 preference structure a priori, without explicit inputs. This highlights the approach’s value
 455 in non-adversarial settings, where subgroup discovery enables tailored treatment strategies.

456 **Historical Comparison.** In contrast to AMCEs, our methods yield *distributions* over
 457 profiles, enabling likelihood-based evaluation of observed candidates. We map the 2016 pri-
 458 mary contenders to the conjoint levels of Ono & Burden (2019) (details in §A.III.1; we make
 459 this historical data on observed candidate features available open source on Hugging Face
 460 (anonymous URL)); when a stance is ambiguous, we average uniformly over plausible lev-
 461 els. Fig. 2 shows that the average-case optimizer (uniform opponent) implies vote shares far
 462 outside the historical two-party range since 1976, whereas the adversarial optimizer closely
 463 matches the 2016 result and its confidence interval covers the historical range. We then score
 464 each 2016 contender by the log probability of their features under the estimated optimal
 465 stochastic interventions. As seen in the table accompanying Fig. 2, log probabilities under
 466 the adversarial strategies are higher than with average-case. Fig. 10 highlights heterogeneity
 467 in polarization. Finally, Fig. A.III.5 aggregates the strategic divergence factor from Eq. 7;
 468 overall, Democratic candidates show somewhat higher divergence.



| Party | Quantity | Mean Log Prob. (s.e.) |
|-------------|----------------------|-----------------------|
| Democrats | Average case | -16.18 (0.62) |
| Democrats | Adversarial case | -16.77 (0.71) |
| Democrats | Log likelihood ratio | -0.59 |
| Republicans | Average case | -15.87 (0.35) |
| Republicans | Adversarial case | -15.77 (0.37) |
| Republicans | Log likelihood ratio | 0.10 |

Figure 2: Comparing the average case and adversarial case results with real historical data. The adversarial case expected optimal outcomes are well within the range of historical experience; the average case outcomes are not.

480 **LIMITATIONS.** This approach has limitations (Table 1). Unlike non-parametric AMCE
 481 estimation, optimal stochastic interventions integrate all factors and strategic dynamics but
 482 rely on a two-step estimator requiring assumptions. While generalizable to complex outcome
 483 models (e.g., neural networks (Zhang et al., 2025)), inference is difficult without accessible
 484 variance-covariance matrices. Uncertainty estimates for equilibrium selection do not account
 485 for preference formation. And, inferred strategic behavior depends on institutional design,
 486 which may be hard to quantify. \square

486 REFERENCES
487

488 Scott F. Abramson, Korhan Koçak, and Asya Magazinnik. What Do We Learn About Voter
489 Preferences from Conjoint Experiments? *American Journal of Political Science*, 66(4):
490 1008–1020, 2022.

491 Scott F. Abramson, Korhan Kocak, Asya Magazinnik, and Anton Strezhnev. Detecting
492 preference cycles in forced-choice conjoint experiments. Preprint, 2023.

493 Susan Athey and Stefan Wager. Policy learning with observational data. *Econometrica*, 89
494 (1):133–161, 2021.

495 Jean-Yves Audibert, Sébastien Bubeck, and Rémi Munos. Best arm identification in multi-
496 armed bandits. In *COLT*, pp. 41–53, 2010.

497 Kirk Bansak, Jens Hainmueller, Daniel J Hopkins, and Teppei Yamamoto. The Number of
498 Choice Tasks and Survey Satisficing in Conjoint Experiments. *Political Analysis*, 26(1):
499 112–119, 2018.

500 Eli Ben-Michael, D. James Greiner, Kosuke Imai, and Zhichao Jiang. Safe policy learn-
501 ing through extrapolation: Application to pre-trial risk assessment. Technical report,
502 arXiv:2109.11679, 2021.

503 Henrik Serup Christensen, Theodora Järvi, Mikko Mattila, and Åsa von Schoultz. How
504 voters choose one out of many: a conjoint analysis of the effects of endorsements on
505 candidate choice. *Political research exchange*, 3(1):1892456, 2021.

506 Brandon de la Cuesta, Naoki Egami, and Kosuke Imai. Experimental design and statistical
507 inference for conjoint analysis: The essential role of population distribution. 2019.

508 Miroslav Dudik, John Langford, and Lihong Li. Doubly Robust Policy Evaluation and
509 Learning. In *Proceedings of the 28th International Conference on Machine Learning*,
510 2011.

511 Naoki Egami and Kosuke Imai. Causal interaction in factorial experiments: Application
512 to conjoint analysis. *Journal of the American Statistical Association*, 114(526):529–540,
513 2019.

514 Fabio Franchino and Francesco Zucchini. Voting in a Multi-dimensional Space: A Conjoint
515 Analysis Employing Valence and Ideology Attributes of Candidates. *Political Science
516 Research and Methods*, 3(2):221–241, 2015.

517 Max Goplerud, Kosuke Imai, and Nicole E Pashley. Estimating heterogeneous causal ef-
518 fects of high-dimensional treatments: Application to conjoint analysis. *arXiv preprint
519 arXiv:2201.01357*, 2022.

520 Jens Hainmueller, Daniel J Hopkins, and Teppei Yamamoto. Causal Inference in Conjoint
521 Analysis: Understanding Multidimensional Choices via Stated Preference Experiments.
522 *Political Analysis*, 22(1):1–30, 2014.

523 Dae Woong Ham, Kosuke Imai, and Lucas Janson. Using machine learning to test causal
524 hypotheses in conjoint analysis. *arXiv preprint arXiv:2201.08343*, 2022.

525 Kosuke Imai and Aaron Strauss. Estimation of Heterogeneous Treatment Effects from
526 Randomized Experiments, with Application to the Optimal Planning of the Get-out-the-
527 vote Campaign. *Political Analysis*, 19(1):1–19, 2011.

528 Nathan Kallus and Angela Zhou. Minimax-optimal Policy Learning under Unobserved
529 Confounding. *Management Science*, 67(5):2870–2890, 2021. doi: 10.1287/mnsc.2020.3699.

530 Patricia A Kirkland and Alexander Coppock. Candidate choice without party labels: New
531 insights from conjoint survey experiments. *Political Behavior*, 40:571–591, 2018.

532 Toru Kitagawa and Aleksey Tetenov. Who should be treated? empirical welfare maximiza-
533 tion methods for treatment choice. *Econometrica*, 86(2):591–616, 2018.

540 David M Kreps. Nash equilibrium. *Game Theory*, pp. 167–177, 1989.
 541

542 Jason D Lee, Max Simchowitz, Michael I Jordan, and Benjamin Recht. Gradient Descent
 543 Only Converges to Minimizers. In *Conference on learning theory*, pp. 1246–1257. PMLR,
 544 2016.

545 Sergey Levine, Aviral Kumar, George Tucker, and Justin Fu. Offline reinforcement learning:
 546 Tutorial, review, and perspectives on open problems. *arXiv preprint arXiv:2005.01643*,
 547 2020.

548 Michael L Littman. Markov games as a framework for multi-agent reinforcement learning.
 549 In *Machine learning proceedings 1994*, pp. 157–163. Elsevier, 1994.

550 Guoer Liu and Yuki Shiraito. Multiple hypothesis testing in conjoint analysis. *Political
 551 Analysis*, pp. 1–16, 2023.

552

553 Tyler Lu, Dávid Pál, and Martin Pál. Contextual Multi-armed Bandits. In *Proceedings
 554 of the Thirteenth International Conference on Artificial Intelligence and Statistics*, pp.
 555 485–492. JMLR Workshop and Conference Proceedings, 2010.

556

557 Yoshikuni Ono and Barry C Burden. The Contingent Effects of Candidate Sex on Voter
 558 Choice. *Political Behavior*, 41:583–607, 2019.

559

560 Yanxia Zhang, Francine Chen, Shabnam Hakimi, Totte Harinen, Alex Filipowicz, Yan-Ying
 561 Chen, Rumen Iliev, Nikos Arechiga, Kalani Murakami, Kent Lyons, et al. Conjointnet:
 562 Enhancing conjoint analysis for preference prediction with representation learning. *arXiv
 563 preprint arXiv:2503.11710*, 2025.

564

565 Yi Zhang, Eli Ben-Michael, and Kosuke Imai. Safe policy learning under regression discon-
 tinuity designs. *arXiv preprint arXiv:2208.13323*, 2022.

566

567 Yingqi Zhao, Donglin Zeng, John A. Rush, and Michael R. Kosorok. Estimating individual-
 568 ized treatment rules using outcome weighted learning. *Journal of the American Statistical
 569 Association*, 107(499):1106–1118, 2012.

570

571

572

573

574

575

576

577

578

579

580

581

582

583

584

585

586

587

588

589

590

591

592

593

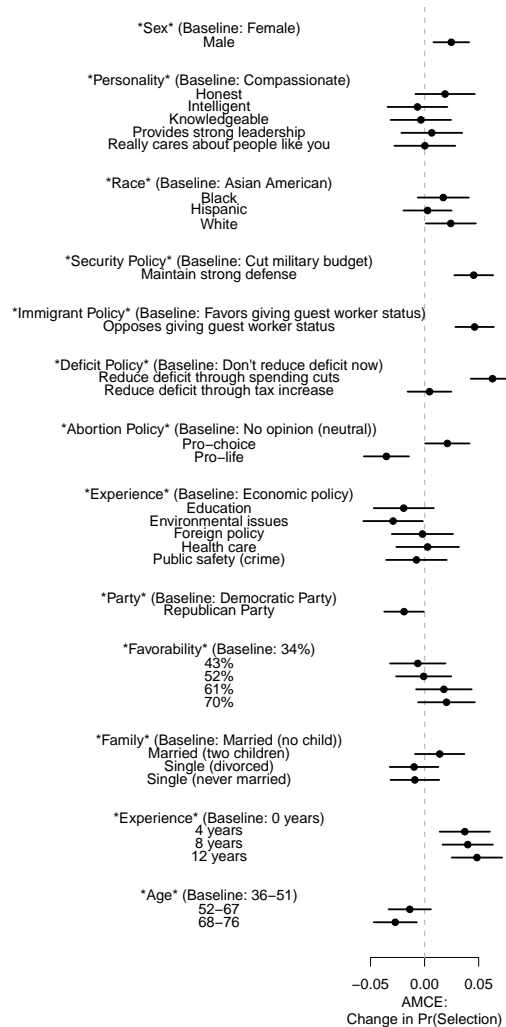
594 MAIN APPENDICES

595 596 A APPENDIX

597 598 A.1 ONO & BURDEN, CONTEXT

600 To fix ideas, we consider a conjoint analysis of candidate choice for the U.S. President,
 601 originally conducted by Ono & Burden (2019). The survey was fielded in March 2016, with
 602 choice of conjoint features influenced by the context of the 2016 US presidential elections.
 603 In this experiment, the outcome is a binary indicator stating whether one hypothetical
 604 candidate or the other was selected by a respondent. Candidate features were randomized
 605 with uniform probability and included age, sex, family context, and race.

606 The authors investigated various AMCEs, with a particular focus on gender. The AMCEs
 607 are computed non-parametrically by taking the difference between the fraction of female
 608 versus male candidates selected, averaging over all other (uniformly allocated) features of
 609 the candidate and its opponent. Fig. 3 summarizes all factor-level AMCEs; the authors
 610 concluded that female candidates are disadvantaged but the effect magnitude is small.



645 Figure 3: An AMCE analysis using presidential candidates from the conjoint data of Ono
 646 & Burden (2019).

648 A.2 METHODOLOGICAL DETAILS
649650 **Certifiability.**
651652 **DEFINITION 1 (RESTRICTED EQUILIBRIUM AND EXPLOITABILITY)** Let $\Pi_{\text{fact}}^A, \Pi_{\text{fact}}^B$ be the
653 factored policy classes. A pair $(\pi^A, \pi^B) \in \Pi_{\text{fact}}^A \times \Pi_{\text{fact}}^B$ is a restricted minimax equilib-
654 rium if it is a saddle point of Q_{inst} when each player is constrained to Π_{fact}^c . Given a
655 candidate pair (π^A, π^B) , define
656

657
$$\epsilon_{\text{ext}}^A = \max_{\sigma \in \Delta(\mathcal{T})} Q_{\text{inst}}(\sigma, \pi^B; \pi^{A'}, \pi^{B'}, \Delta) - Q_{\text{inst}}(\pi^A, \pi^B; \pi^{A'}, \pi^{B'}, \Delta),$$

658

659
$$\epsilon_{\text{ext}}^B = Q_{\text{inst}}(\pi^A, \pi^B; \pi^{A'}, \pi^{B'}, \Delta) - \min_{\sigma \in \Delta(\mathcal{T})} Q_{\text{inst}}(\pi^A, \sigma; \pi^{A'}, \pi^{B'}, \Delta).$$

660

661 The external exploitability is $\epsilon_{\text{ext}} = \max\{\epsilon_{\text{ext}}^A, \epsilon_{\text{ext}}^B\}$; $\epsilon_{\text{ext}} = 0$ certifies a full mixed-strategy
662 equilibrium.
663664 Next, we show that when the opponent’s strategy is fixed, the institution-aware payoff is
665 linear in the focal player’s joint distribution, so the focal player’s best response (over the
666 full simplex) is always a pure profile and can be found by simply evaluating a scalar score
667 for each profile. This lets us compute exploitability exactly (or by approximation) without
668 solving an inner optimization.
669670 **PROPOSITION 2 (LINEARITY)** Fix $\pi^{A'}, \pi^{B'}, \Delta$ and π^B . Then $Q_{\text{inst}}(\pi^A, \pi^B)$ is linear in
671 π^A . Specifically,

672
$$Q_{\text{inst}}(\pi^A, \pi^B) = \sum_{\mathbf{t} \in \mathcal{T}} \pi^A(\mathbf{t}) G^A(\mathbf{t}),$$

673

674 where $V(\mathbf{t}, \mathbf{u})$ denotes the general-election win probability for A when nominees \mathbf{t} and \mathbf{u} face
675 off:

676
$$V(\mathbf{t}, \mathbf{u}) := \mathbb{E}_{i \in \mathcal{E}}[C(\mathbf{t}, \mathbf{u})] = \Pr_{i \in \mathcal{E}}(Y_i(\mathbf{t}) > Y_i(\mathbf{u}))$$

677

678 and

679
$$\Psi^B(\mathbf{t}) = \sum_{\mathbf{u}} \bar{\pi}^B(\mathbf{u}) V(\mathbf{t}, \mathbf{u}), \quad G^A(\mathbf{t}) = \sum_{\mathbf{s}} \pi^{A'}(\mathbf{s}) \left\{ \Psi^B(\mathbf{t}) \kappa_A(\mathbf{t}, \mathbf{s}) + \Psi^B(\mathbf{s}) [1 - \kappa_A(\mathbf{t}, \mathbf{s})] \right\},$$

680

681 as the expected general-election win probability for A if A nominates profile \mathbf{t} and B ’s nomi-
682 nee is drawn from its post-primary distribution $\bar{\pi}^B$ (which itself reflects the primary rules
683 Δ). Hence a full-simplex best response for A is the pure profile $\mathbf{t}^* \in \arg \max_{\mathbf{t}} G^A(\mathbf{t})$, and
684 $\epsilon_{\text{ext}}^A = \max_{\mathbf{t}} G^A(\mathbf{t}) - \sum_{\mathbf{t}} \pi^A(\mathbf{t}) G^A(\mathbf{t})$. The symmetric statement holds for B .
685686 *Proof sketch.* Substitute the primary pushforward (Eq. 4) into Q_{inst} and collect terms in
687 π^A .
688689 **Covariate-Sensitive Strategies** The approach discussed here can accommodate respon-
690 dent covariates, as is possible in the sequential decision-making context (Lu et al., 2010). In
691 our discussion up to now, the new treatment probabilities were assigned without considering
692 the specific characteristics of each respondent. We could consider stochastic interventions
693 that took into account covariate information in the targeting of the high-dimensional treat-
694 ments:
695

696
$$Q(\pi^*) = \max_{\pi} Q(\pi) = \max_{\pi} \mathbb{E}_{\mathbf{X}} [\mathbb{E}_{Y|\mathbf{X}} [Y_i(\mathbf{t}) \mid \mathbf{X}_i = \mathbf{x}] \Pr_{\pi}(\mathbf{T}_i = \mathbf{t} \mid \mathbf{X}_i = \mathbf{x})]$$

697
$$= \max_{\pi} \left\{ \sum_{\mathbf{x}} \sum_{\mathbf{t} \in \mathcal{T}} \mathbb{E}[Y_i(\mathbf{t}) \mid \mathbf{X}_i = \mathbf{x}] \Pr_{\pi}(\mathbf{T}_i = \mathbf{t} \mid \mathbf{X}_i = \mathbf{x}) \Pr(\mathbf{X}_i = \mathbf{x}) \right\}.$$

698

699 The covariate-sensitive distribution, $\Pr_{\pi}(\mathbf{T}_i \mid \mathbf{X}_i)$, can be operationalized by having different
700 factor-level probabilities for each cluster, with a model predicting the cluster probabilities for
701

702 each unit. If we let π_{dlk} denote the probability of factor d , level l , for cluster $k \in \{1, \dots, K\}$:

$$\begin{aligned}
 704 \quad \Pr_{\boldsymbol{\pi}}(\mathbf{T}_i | \mathbf{X}_i) &= \sum_{k=1}^K \Pr_{\boldsymbol{\pi}_k}(\mathbf{T}_i | Z_{ik} = 1) \Pr(Z_{ik} = 1 | \mathbf{X}_i) \\
 705 \\
 706 \quad &= \sum_{k=1}^K \underbrace{\left\{ \prod_{d=1}^D \Pr_{\boldsymbol{\pi}_k}(T_{id} | Z_{ik} = 1) \right\}}_{\text{Categorical probabilities for cluster } k} \underbrace{\Pr(Z_{ik} = 1 | \mathbf{X}_i = \mathbf{x})}_{\text{Softmax regression}}
 \end{aligned} \tag{8}$$

710
711 In this context, estimation can be conducted using outcome models that cluster main and
712 interaction effects (Goplerud et al., 2022).

713 A.3 SIMULATION DETAILS, AVERAGE CASE

714
715 **Simulation Design: Average Case.** To probe finite-sample dynamics of the proposed
716 optimal stochastic intervention methodologies for conjoint analysis, we employ Monte Carlo
717 methods. In our simulations, we analyze synthetic factorial experiments with binary treat-
718 ments where each treatment is drawn from an independent Bernoulli with probability pa-
719 rameter 0.5. We adopt a linear outcome model with interactions³:

$$720 \quad Y_i(\mathbf{T}_i) = \beta_0 + \sum_{d=1}^D \sum_{l=1}^{L_d-1} \beta'_{dl} \mathbb{I}\{T_{id} = l\} + \sum_{d', d'': d < d'} \sum_{l'=1}^{L_{d'}-1} \sum_{l''=1}^{L_{d''}-1} \gamma_{d', d''} \mathbb{I}\{T_{id'} = l'\} \mathbb{I}\{T_{id''} = l''\} + \epsilon_i,$$

721
722 with $\epsilon_i \sim N(0, 0.1)$, since this makes the computation of $Q(\boldsymbol{\theta})$ straightforward (in particular,
723 $Q(\boldsymbol{\pi}) = \beta' \boldsymbol{\pi} + \sum_{d, d': d < d'} \gamma_{d, d'} \pi_d \pi_{d'}$). The coefficients are drawn i.i.d. from $N(0, 1)$, and the
724 interaction coefficients are scaled so that the R^2 in using the main effects only to predict
725 the outcome is 0.70 (ensuring some effective non-linearity). We obtain the true value of $\boldsymbol{\pi}^*$
726 fixing λ and solving for $\boldsymbol{\pi}^*$ using Proposition 1.

727
728 To analyze finite sample convergence of $\hat{\boldsymbol{\pi}}^*$, we vary the number of observations, $n \in$
729 $\{500, 1500, 3500, 10000\}$. To analyze performance in the high-dimensional setting, where
730 the number of treatment combinations is greater than the number of observations, we vary
731 the number of factors, $K \in \{5, 10, 20\}$. We fix λ so that the regularized optimal stochas-
732 tic interventions have no factor probabilities greater than 0.9, while having a degree of
733 divergence from the (uniform) data-generating probabilities.

734
735 **Simulation Results: Average Case.** First, we examine the degree to which $\hat{\boldsymbol{\pi}}^*$, the
736 optimal stochastic intervention factor probabilities, and $\hat{Q}(\hat{\boldsymbol{\pi}}^*)$, the average outcome under
737 the regularized stochastic intervention, converge to the true values as the sample size grows.
738 We see in the left panel of Fig. 4 that, with a small number of factors (5), the bias of $\hat{\boldsymbol{\pi}}^*$
739 is insignificant even with a small sample size (500). The variance of estimation contributes
740 more prominently to the overall RMSE for all numbers of covariates; the variance decreases
741 rapidly with the sample size. We see a similar pattern for $\hat{Q}(\hat{\boldsymbol{\pi}}^*)$ in right panel of Fig.
742 4, where the bias is nominal with a small number of factors and the variance contributes
743 more prominently to the overall RMSE, which still decreases with the sample size. Results
744 are consistent with the idea that the optimal stochastic interventions are more difficult to
745 estimate if there are more candidate features involved.

746
747 We next compare the value of the optimal stochastic intervention, $Q(\hat{\boldsymbol{\pi}}^*)$, against a simple
748 baseline policy that, for each factor, places all mass on the level with the highest estimated
749 main effect from a main-effects-only model (i.e., a degenerate policy selecting per-factor
750 AMCE maximizers, ignoring interactions). As shown in Figure 5, the optimal SI method
751 yields a higher mean value of 1.550 compared to the baseline, demonstrating the benefits of
752 accounting for interactions in policy optimization.

753
754 We next consider estimated uncertainties compared against true sampling uncertainties.
755 We see in Fig. A.I.1 that the asymptotic variance of $\hat{Q}(\hat{\boldsymbol{\pi}}^*)$ is somewhat underestimated

³For simplicity, we here do not adopt the sum-to-0 coefficient constraint, and instead use a baseline category.

756 Table 1: Comparing different approaches to conjoint analysis. \Pr here refers to the data-
 757 generating probability distribution over candidate features; \Pr_{π} refers to the distribution
 758 defining an optimal stochastic intervention. SI denotes “stochastic intervention”; GLM
 759 denotes “generalized linear model.”

| | <i>Average Marginal Component Effect (AMCE)</i> | <i>Average Marginal Interaction Effect (AMIE)</i> | <i>Average Case Optimal Stochastic Intervention</i> | <i>Adversarial Case Optimal Stochastic Intervention</i> |
|---|---|---|--|--|
| <i>Character</i> | | | | |
| Components considered at a time | 1 | 2+ | All | All |
| Baseline factor category specified? | Yes | Yes | No | No |
| Marginalization over: | Respondents; other factors of reference profile via \Pr ; all factors of opponent profile via \Pr | Respondents; other factors of reference profile via \Pr ; all factors of opponent profile via \Pr | Respondents; factors of reference via \Pr_{π} , opponent profile via \Pr | Respondents; factors of reference via \Pr_{π^a} , opponent profile via \Pr_{π^b} |
| Informative about strategy in an adversarial setting? | No | No | No | Yes |
| Hyper-parameters | Strength of regularization in outcome model (rarely used) | Strength of regularization in outcome model if used | Strength of regularization in outcome model; SI regularization | Strength of regularization in outcome model; SI regularization |
| Uncertainty estimation | GLM variance-covariance; bootstrap | GLM variance-covariance; bootstrap | GLM variance-covariance + Delta method | GLM variance-covariance + Delta method |
| <i>Data Requirements</i> | | | | |
| Requires forced-choice design? | No | No | No | Yes |
| Requires distinct respondent and profile sub-groups? | No | No | No | Yes |

800 for small sample sizes. Fig. A.I.2 in §A.I.8 reports the true sampling variability of $\hat{\pi}^*$
 801 against the average standard error estimate from asymptotic inference; estimates are neither
 802 systematically too wide nor too narrow. Finally, we examine coverage, which combines
 803 information about point with variance estimates. We see in Fig. 8 coverage close to the
 804 target coverage rate across the number of factors and observations for the components of
 805 π^* and (in Fig. 9) for $\hat{Q}(\hat{\pi}^*)$ itself.

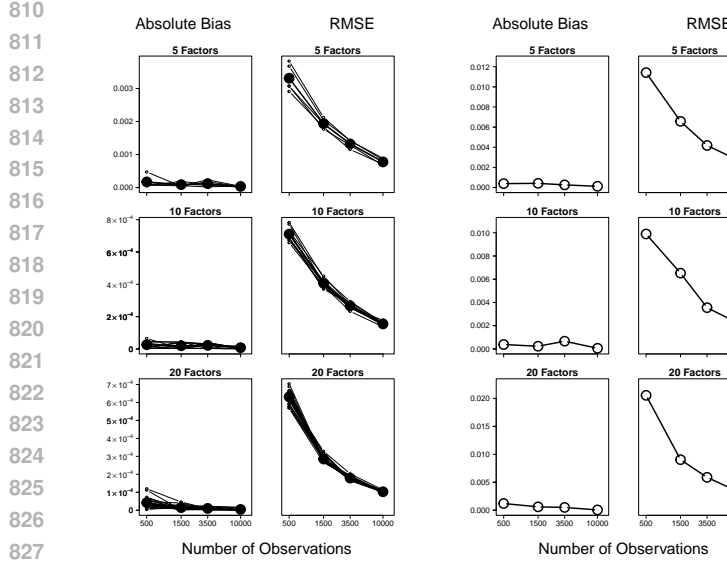


Figure 4: LEFT. Estimation bias and RMSE of π^* . Each line represents one entry in π^* . The bold line and closed circles represent the average value.
RIGHT. The estimation bias and RMSE of $Q(\pi^*)$.

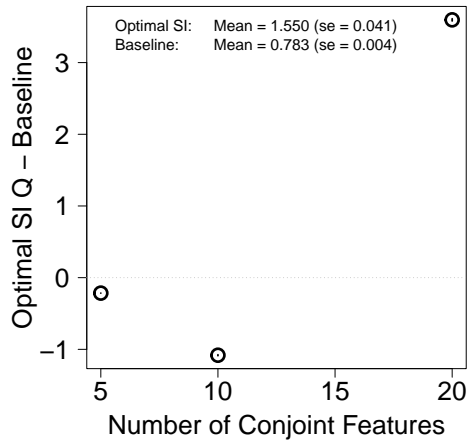


Figure 5: Comparison against a baseline.

A.4 SIMULATION DESIGN: ADVERSARIAL CASE

In order to investigate finite-sample performance under the more complex adversarial setting, we simulate strategic behavior between two hypothetical political parties denoted by R (Republican) and D (Democrat). We design a two-stage electoral process in which each party first selects a nominee via a primary election, and then those nominees compete in a general election. Voters differ by party affiliation, which determines whether they participate in the corresponding primary. Let p_R denote the fraction of Republican voters in the electorate, so that $p_D = 1 - p_R$ is the fraction of Democratic voters. For each simulation run, we fix $p_R \in \{0.2, 0.3, 0.5, 0.65, 0.8\}$ along a grid, and we vary the conjoint sample size $n \in \{1000, 5000, 10000\}$. Each grid cell is replicated across Monte Carlo draws.

Within each simulated dataset, we generate responses for primary and general-election stages. In the first stage, only voters from party R or party D participate in their own party's primary. We assign two potential candidate profiles for party R and two for party D ; one of these candidates is selected using the party's assignment mechanism, the other uniformly. Let these be $\mathbf{T}_i^{R,1}, \mathbf{T}_i^{R,2}$ for R and $\mathbf{T}_i^{D,1}, \mathbf{T}_i^{D,2}$ for D . We specify probabilities with which

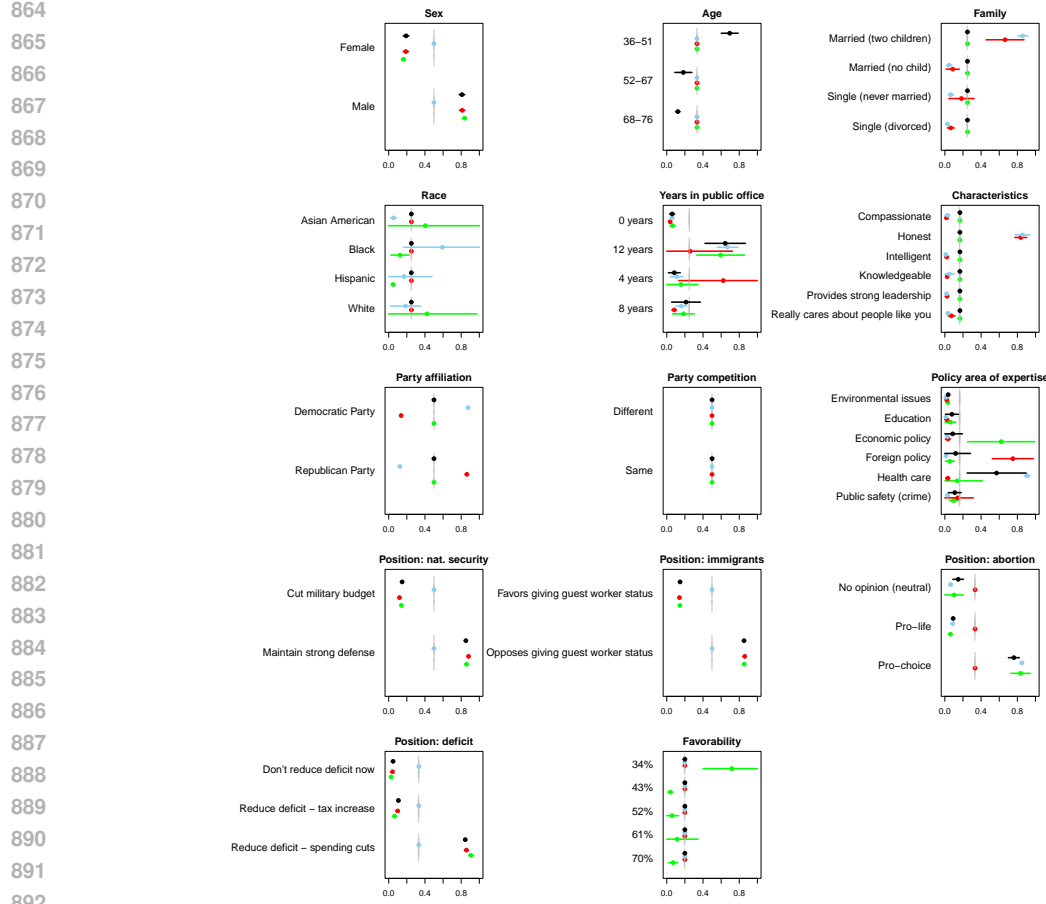


Figure 6: Optimal strategies in the average case setting. Black, blue, red, and green denote the average case optimal among all, Democrat, Republican, and Independent respondents in the sample.

each candidate profile is chosen by each respondent in that primary, using logistic models to capture how voters respond to candidate features—here, simply gender for tractability when computing ground truth equilibria via grid search. In the second stage, *all* voters, R and D , face a forced choice in the general election between $\mathbf{T}_i^{R,*}$ and $\mathbf{T}_i^{D,*}$, winners of the respective primaries. In the second stage, Republican and Democrat voters select candidates again using two logistic models.

Having outlined the data-generating process, we now discuss how we compute the ground-truth strategies approximating a Nash equilibrium in the space of possible profile distributions for each party. The quantities π^R and π^D describes a mixed strategy over candidate characteristics for R and D , respectively. We define

$$Q(\pi^R, \pi^D) = \mathbb{E}_{\mathbf{T}_i^R \sim \pi^R, \mathbf{T}_i^D \sim \pi^D} [\Pr(Y_i(\mathbf{T}_i^R) > Y_i(\mathbf{T}_i^D))],$$

where \mathbf{T}_i^R and \mathbf{T}_i^D represent each party's selection (who competes against the primary challenger). To find a Nash equilibrium, we compute each party's best response to the other via a discrete grid search. In practice, this means we scan over π^R and π^D , computing

$$\max_{\pi^R} \min_{\pi^D} Q(\pi^R, \pi^D) = \min_{\pi^D} \max_{\pi^R} Q(\pi^R, \pi^D),$$

checking which (π^R, π^D) satisfies the equilibrium condition that neither party can unilaterally improve its expected vote share; we label these as the equilibrium strategies.

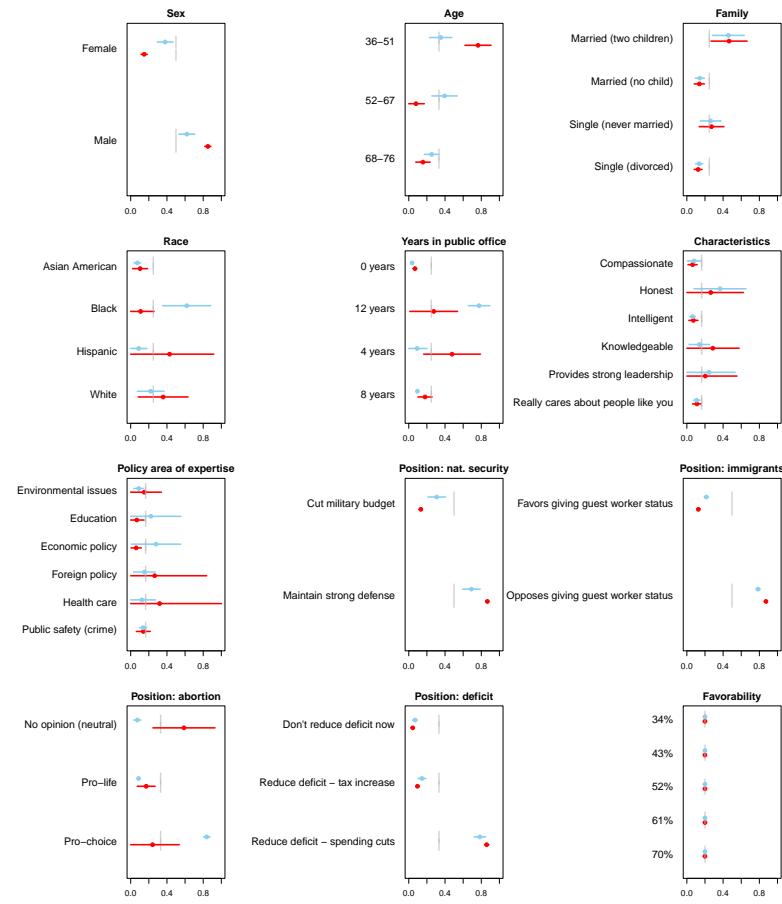
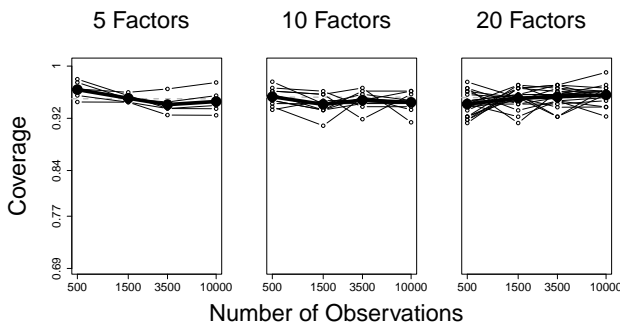


Figure 7: Optimal strategies in an adversarial setting. Blue/red denote the equilibrium strategy for the agent facing Democratic/Republican voters in the primary stage, respectively.

In order to evaluate the finite-sample performance of the proposed algorithm for the adversarial setting, we implemented the two-stage design described in the preceding section while varying the proportion of Republican voters, p_R , in the electorate. That is, for each Monte Carlo run, we save the estimated equilibrium distribution for π^R and π^D , along with the realized general-election outcomes under those strategies. By aggregating results across the grid of $\{p_R, n_{\text{obs}}\}$ and across replications, we examine trends in how party composition p_R and sample size n_{obs} affect equilibrium strategies, estimated vote shares, and convergence. This design allows us to evaluate the proposed adversarial methodology under changing population compositions and sample sizes. We focus on summarizing estimation accuracy for π^R : we record root-mean-squared error (RMSE) and coverage of confidence intervals under repeated sampling, with coverage targeting the nominal rate of 95%.

A.5 EMPIRICAL RESULTS REFERENCED IN MAIN TEXT



991 Figure 8: Finite-sample coverage of π^* . Each line represents one entry in π^* . The bold line
992 and closed circles represent the average value.

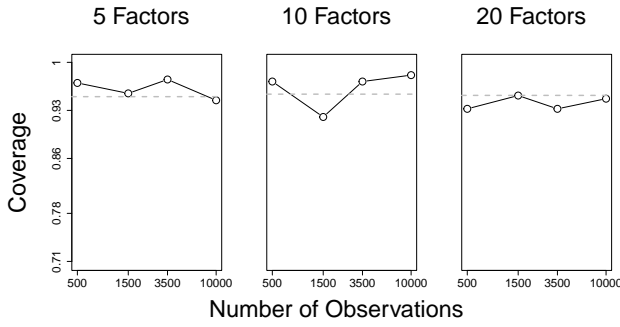
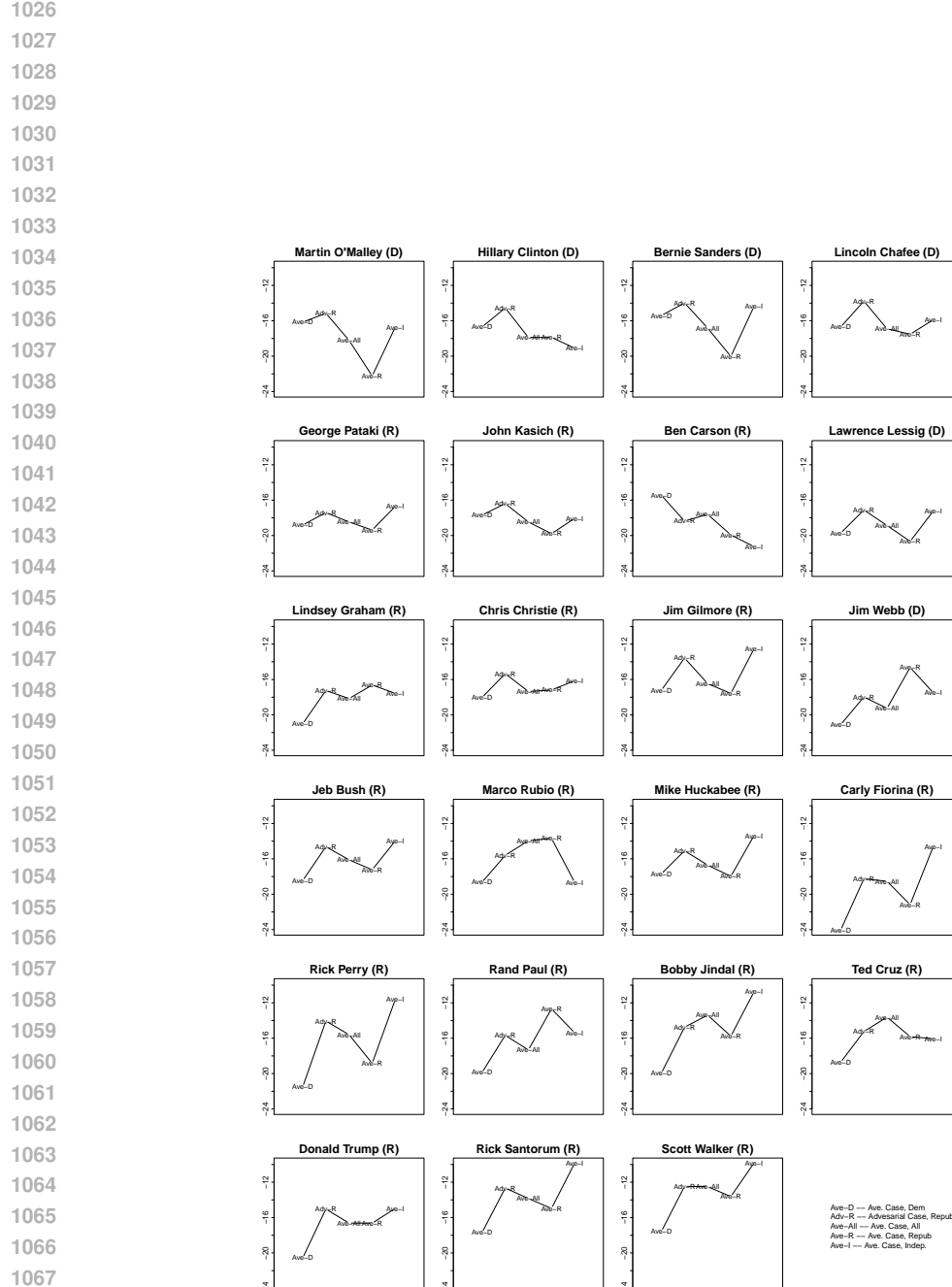


Figure 9: Finite-sample coverage for $Q(\pi^*)$.



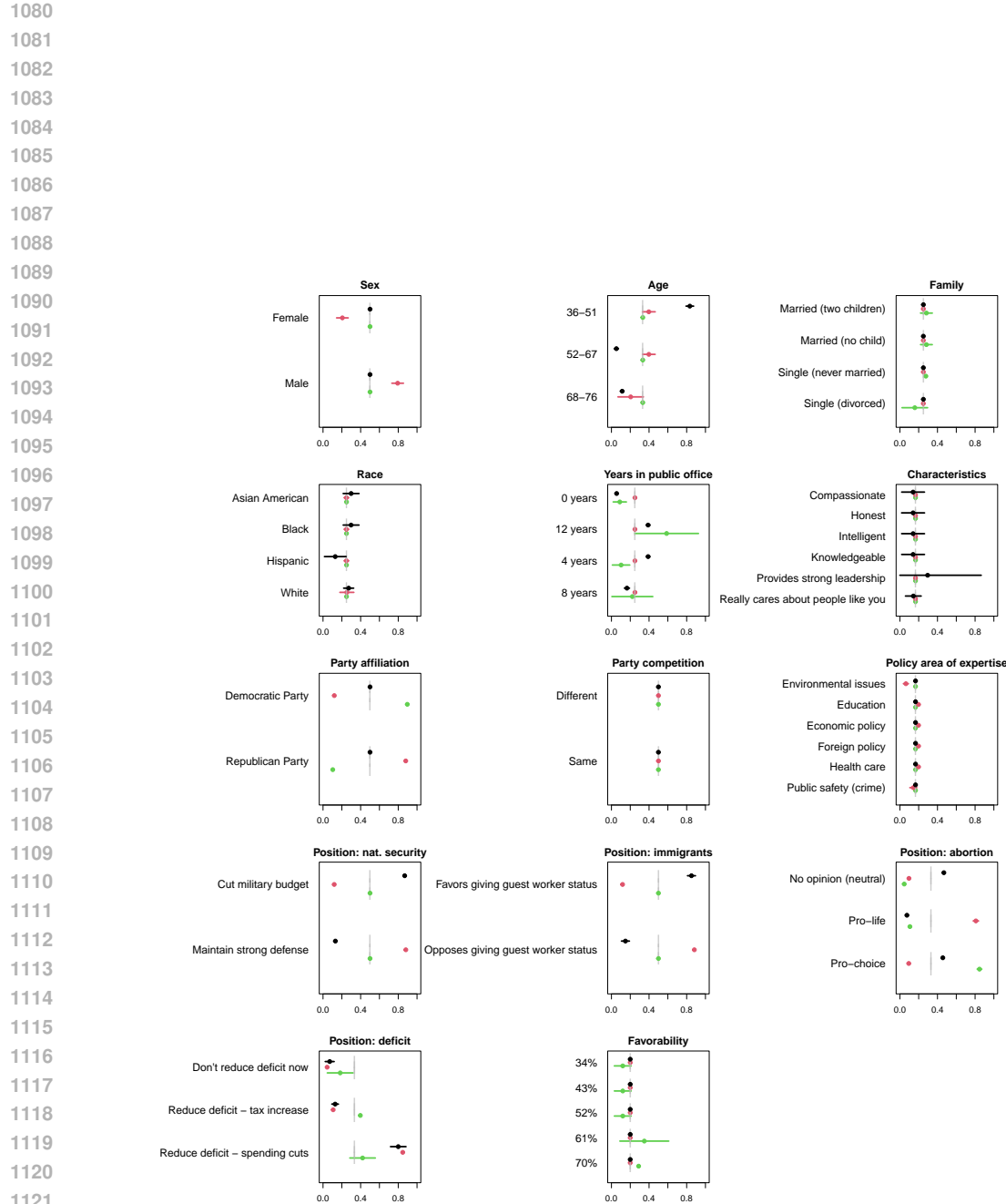


Figure 11: Optimal strategies in the covariate sensitive case, where a different strategy for allocating candidate features can be used for three data-derived clusters of voters.

1134 SUPPLEMENTARY APPENDICES
11351136 APPENDIX I: THEORETICAL ANALYSIS
11371139 A.I.1 THE OPTIMAL STOCHASTIC INTERVENTION IN A TWO-WAY INTERACTION
1140 MODEL WITH BINARY FACTORS1141 Recall that the objective function to maximize is
1142

1143
$$O(\boldsymbol{\pi}) = Q(\boldsymbol{\pi}) - \lambda \|\mathbf{p} - \boldsymbol{\pi}\|^2$$

1144
$$= \beta_0 + \sum_{d=1}^D \beta_d \pi_d + \sum_{d' < d''} \gamma_{d', d'} \pi_{d'} \pi_{d''} - \lambda \sum_{d'''=1}^D \{(\pi_{d'''} - p_{d'''})^2 + ([1 - \pi_{d'''}] - [1 - p_{d'''}])^2\}$$

1145

1146 so that
1147

1148
$$\frac{dO}{d\pi_d} = \beta_d + \sum_{d, d'' \neq d'} \gamma_{d, d'} \pi'_d - 4\lambda(\pi_d - p_d) = 0$$

1149
$$\implies$$

1150
$$\sum_{d, d' \neq d} \gamma_{d, d'} \pi_{d''} - 4\lambda \pi_d = -\beta_d - 4\lambda p_d$$

1151

1152 where we use \mathbf{p}_d to denote the vector of Categorical probabilities for all levels in factor d .
1153 This sets up a system of D linear equations with D unknowns, which can be represented in
1154 matrix form:
1155

1156
$$\mathbf{C}\boldsymbol{\pi}^* = \mathbf{B}$$

1157
$$\boldsymbol{\pi}^* = \mathbf{C}^{-1}\mathbf{B},$$

1158

1159 where $B_{d,1} = -\beta_d - 4\lambda p_d$, $C_{d,d} = -4\lambda$ and $C_{d,d''} = \gamma_{d,d''}$.
11601161 A.I.2 THE OPTIMAL STOCHASTIC INTERVENTION IN A TWO-WAY INTERACTION
1162 MODEL WITH MULTIPLE FACTOR LEVELS
11631164 The outcome model with multiple factor levels is
1165

1166
$$Y_i(t) = \beta_0 + \sum_{d=1}^D \sum_{l=1}^{L_d-1} \beta_{dl} t_{dl} + \sum_{d', d''; d' < d''} \sum_{l'=1}^{L_{d'}-1} \sum_{l''=1}^{L_{d''}-1} \gamma_{d', l', d'', l''} t_{d', l'} t_{d'', l''} + \epsilon_i,$$

1167

1168 where t_{dl} denotes the binary indicator for whether level l in factor d is assigned. By linearity
1169 of expectations and independence of factors:
1170

1171
$$Q(\boldsymbol{\pi}) = \beta_0 + \sum_{d=1}^D \sum_{l=1}^{L_d-1} \beta_{dl} \pi_{dl} + \sum_{d', d''; d' < d''} \sum_{l'=1}^{L_{d'}-1} \sum_{l''=1}^{L_{d''}-1} \gamma_{d', l', d'', l''} \pi_{d', l'} \pi_{d'', l''}.$$

1172

1173 The objective is now
1174

1175
$$O(\boldsymbol{\pi}) = Q(\boldsymbol{\pi}) - \lambda \|\mathbf{p} - \boldsymbol{\pi}\|^2$$

1176
$$= \beta_0 + \sum_{d=1}^D \sum_{l=1}^{L_d-1} \beta_{dl} \pi_{dl} + \sum_{d', d''; d' < d''} \sum_{l'=1}^{L_{d'}-1} \sum_{l''=1}^{L_{d''}-1} \gamma_{d', l', d'', l''} \pi_{d', l'} \pi_{d'', l''}$$

1177
$$- \lambda \sum_{d'''=1}^D \left\{ \sum_{l'''=1}^{L_{d'''}-1} (\pi_{d''', l'''} - p_{d''', l'''})^2 + \left(1 - \left[\sum_{l'''=1}^{L_{d'''}-1} \pi_{d''', l'''} \right] - \left(1 - \left[\sum_{l'''=1}^{L_{d'''}-1} p_{d''', l'''} \right] \right) \right)^2 \right\}$$

1178

1188 so that, for $l < L_d$:

$$\begin{aligned}
 1190 \quad \frac{dO}{d\pi_{dl}} &= \beta_{dl} + \sum_{d,d' \neq d} \sum_{l=1}^{L_d-1} \sum_{l'=1}^{L_{d'}-1} \gamma_{dl,d'l'} \pi_{d'l'} - 2\lambda(\pi_{dl} - p_{dl}) - 2\lambda \left(\sum_{l'=1}^{L_d-1} (\pi_{dl'} - p_{dl'}) \right) = 0 \\
 1193 \quad \implies \\
 1194 \quad \sum_{d,d' \neq d} \sum_{l=1}^{L_d-1} \sum_{l'=1}^{L_{d'}-1} \gamma_{dl,d'l'} \pi_{d'l'} - 4\lambda\pi_{dl} - 2\lambda \sum_{l' \neq l, l' < L_d} \pi_{dl'} &= -\beta_{dl} - 4\lambda p_{dl} - 2\lambda \sum_{l' \neq l, l' < L_d} p_{dl'}
 \end{aligned}$$

1198 with This again sets up a system of $\sum_{d=1}^D (L_d - 1)$ linear equations with the same number
1199 of unknowns, which can be represented in matrix form:

$$\begin{aligned}
 1200 \quad \mathbf{C}\boldsymbol{\pi}^* &= \mathbf{B} \\
 1201 \quad \boldsymbol{\pi}^* &= \mathbf{C}^{-1}\mathbf{B}.
 \end{aligned}$$

1203 where, letting $r(\cdot)$ denote a function returning the appropriate index into the matrix
1204 rows/columns:

$$\begin{aligned}
 1206 \quad B_{r(dl),1} &= -\beta_{dl} - 4\lambda p_{dl} - 2\lambda \sum_{l' \neq l, l' < L_d} p_{dl'} \\
 1207 \\
 1208 \quad C_{r(dl),r(dl)} &= -4\lambda \\
 1209 \quad C_{r(dl),r(dl')} &= -2\lambda \\
 1210 \quad C_{r(dl),r(d'l'')} &= \gamma_{dl,d'l''}
 \end{aligned}$$

1212 A.I.3 THE OPTIMAL STOCHASTIC INTERVENTION IN A TWO-WAY INTERACTION 1213 MODEL UNDER FORCED CHOICE OUTCOMES

1215 The outcome model with multiple factor levels is

$$\begin{aligned}
 1217 \quad \Pr(Y_i(\mathbf{T}_i^a) > Y_i(\mathbf{T}_i^b) \mid \mathbf{T}_i^a, \mathbf{T}_i^b) &= \tilde{\mu} + \sum_{d=1}^D \sum_{l=1}^{L_d} \beta_{dl} (\mathbb{I}\{T_{id}^a = l\} - \mathbb{I}\{T_{id}^b = l\}) \\
 1218 \\
 1219 \quad + \sum_{d',d'':d' < d''} \sum_{l'=1}^{L_{d'}} \sum_{l''=1}^{L_{d''}} \gamma_{d'l',d''l''} (\mathbb{I}\{T_{id'}^a = l', T_{id''}^a = l''\} - \mathbb{I}\{T_{id'}^b = l', T_{id''}^b = l''\}) + \epsilon_i,
 \end{aligned}$$

1223 where t_{dl} denotes the binary indicator for whether level l in factor d is assigned. By linearity
1224 of expectations and independence of factors:

$$\begin{aligned}
 1226 \quad Q(\boldsymbol{\pi}^a, \boldsymbol{\pi}^b) &= \mathbb{E}_{\boldsymbol{\pi}^a(\mathbf{T}_i^a), \boldsymbol{\pi}^b(\mathbf{T}_i^b)} \left[\Pr(Y_i(\mathbf{T}_i^a) > Y_i(\mathbf{T}_i^b) \mid \mathbf{T}_i^a, \mathbf{T}_i^b) \right] \\
 1227 \\
 1228 \quad = \tilde{\mu} + \sum_{d=1}^D \sum_{l=1}^{L_d} \beta_{dl} (\pi_{dl}^* - \pi_{dl}^b) \\
 1229 \\
 1230 \quad + \sum_{d',d'':d' < d''} \sum_{l'=1}^{L_{d'}} \sum_{l''=1}^{L_{d''}} \gamma_{d'l',d''l''} (\pi_{d'l'}^* \pi_{d''l''}^* - \pi_{d'l'}^b \pi_{d''l''}^b)
 \end{aligned}$$

- 1234 • Case 0: Choose $\boldsymbol{\pi}^a$ and $\boldsymbol{\pi}^b$ jointly to maximize the selection probability for \mathbf{T}_i^a .
1235 Problem: Not an interpretable solution: Choose best candidate strategy A to go
1236 against worst possible candidate B .
- 1238 • Case 1: Average Case Analysis: Set $\boldsymbol{\pi}^b$ to be \mathbf{p} . Interpretation: Best candidate
1239 strategy A uniformly averaging over all possible candidate B 's.
- 1240 • Case 2: Minimax Analysis: Set $\boldsymbol{\pi}^a$ to maximize, $\boldsymbol{\pi}^b$ to minimize objective. In-
1241 terpretation: Optimally select candidate strategy A to compete against optimally
selected candidate strategy B .

1242

The objective is now

1243

$$\begin{aligned}
O(\boldsymbol{\pi}^a, \boldsymbol{\pi}^b) &= Q(\boldsymbol{\pi}^a, \boldsymbol{\pi}^b) - \lambda (||\mathbf{p} - \boldsymbol{\pi}^a||^2 + ||\mathbf{p} - \boldsymbol{\pi}^b||^2) \\
&= \tilde{\mu} + \sum_{d=1}^D \sum_{l=1}^{L_d} \beta_{dl} (\pi_{dl}^* - \pi_{dl}^b) \\
&+ \sum_{d', d'': d' < d''} \sum_{l'=1}^{L_{d'}} \sum_{l''=1}^{L_{d''}} \gamma_{d'l', d''l''} (\pi_{d'l'}^* \pi_{d''l''}^* - \pi_{d'l'}^b \pi_{d''l''}^b) \\
&- \lambda \sum_{\#\in\{*,b\}} \sum_{d'''=1}^D \left\{ \sum_{l'''=1}^{L_d} (\pi_{d'''l'''}^{\#} - p_{d'''l'''}^{\#})^2 \right\}
\end{aligned}$$

1244

Under the Average Case Maximizer:

1245

$$\begin{aligned}
O(\boldsymbol{\pi}^a, \mathbf{p}) &= \tilde{\mu} + \sum_{d=1}^D \sum_{l=1}^{L_d} \beta_{dl} (\pi_{dl}^* - p_{dl}) \\
&+ \sum_{d', d'': d' < d''} \sum_{l'=1}^{L_{d'}} \sum_{l''=1}^{L_{d''}} \gamma_{d'l', d''l''} (\pi_{d'l'}^* \pi_{d''l''}^* - p_{d'l'} p_{d''l''}) \\
&- \lambda \sum_{d'''=1}^D \left\{ \sum_{l'''=1}^{L_d} (\pi_{d'''l'''}^* - p_{d'''l'''}^*)^2 \right\}
\end{aligned}$$

1246

so that

1247

$$\begin{aligned}
\frac{dO}{d\pi_{dl}^*} &= \beta_{dl} + \sum_{d, d' \neq d} \sum_{l=1}^{L_d} \sum_{l'=1}^{L_{d'}} \gamma_{dl, d'l'} \pi_{d'l'}^* - 2\lambda(\pi_{dl}^* - p_{dl}) = 0 \\
&\implies \\
&\sum_{d, d' \neq d} \sum_{l=1}^{L_d} \sum_{l'=1}^{L_{d'}} \gamma_{dl, d'l'} \pi_{d'l'}^* - 2\lambda\pi_{dl}^* = -\beta_{dl} - 2\lambda p_{dl}
\end{aligned}$$

1248

This sets up a system of $\sum_{d=1}^D L_d$ linear equations with the same number of unknowns, which can be represented in matrix form:

1249

$$\mathbf{C}\boldsymbol{\pi}^* = \mathbf{B}$$

1250

$$\boldsymbol{\pi}^* = \mathbf{C}^{-1}\mathbf{B}.$$

1251

where, letting $r(\cdot)$ denote a function returning the correct index into the matrix:

1252

$$B_{r(dl),1} = -\beta_{dl} - 2\lambda p_{dl}$$

1253

$$C_{r(dl),r(dl)} = -2\lambda$$

1254

$$C_{r(dl),r(dl')} = 0$$

1255

$$C_{r(dl),r(d'l'')} = \gamma_{dl,d'l''}$$

1256

Here, the optimal stochastic intervention is a deterministic function of the outcome model parameters. The parameters defining the outcome model, $\boldsymbol{\beta}$ and $\boldsymbol{\gamma}$, are not known *a priori*, but can be estimated via generalized linear methods, with the asymptotic standard errors then employed. Because the parameters, $\boldsymbol{\pi}^a$, that define $\Pr_{\boldsymbol{\pi}}^a$ are a deterministic function of the regression parameters, the variance-covariance matrix of $\{\widehat{Q}(\widehat{\boldsymbol{\pi}}^a), \widehat{\boldsymbol{\pi}}^a\}$ can be obtained via the delta method:

1257

$$\text{Var-Cov}(\{\widehat{Q}(\widehat{\boldsymbol{\pi}}^a), \widehat{\boldsymbol{\pi}}^a\}) = \mathbf{J} \widehat{\Sigma} \mathbf{J}',$$

1258

where $\widehat{\Sigma}$ is the variance-covariance matrix from the modeling strategy for Y_i using regression parameters $\boldsymbol{\beta}$ and $\boldsymbol{\gamma}$ and \mathbf{J} is the Jacobian of partial derivatives (e.g., of $\widehat{Q}(\widehat{\boldsymbol{\pi}}^a)$ and $\widehat{\boldsymbol{\pi}}^a$ with respect to the outcome model parameters):

1259

$$\mathbf{J} = \nabla_{\{\widehat{\boldsymbol{\beta}}, \widehat{\boldsymbol{\gamma}}\}} \{\widehat{Q}(\widehat{\boldsymbol{\pi}}^a), \widehat{\boldsymbol{\pi}}^a\}.$$

1296 If the assumptions of the first-stage model hold, then
 1297

$$1298 \sqrt{n} \left(\{\widehat{Q}(\widehat{\boldsymbol{\pi}}^a), \widehat{\boldsymbol{\pi}}^a\} - \{Q(\boldsymbol{\pi}^a), \boldsymbol{\pi}^a\} \right) \rightarrow \mathcal{N}(\mathbf{0}, \mathbf{J} \Sigma_n \mathbf{J}')$$

1300
 1301 A.I.4 GRADIENTS FOR OBTAINING THE VARIANCE-CONSTRAINED OPTIMAL
 1302 STOCHASTIC INTERVENTION IN THE TWO-WAY CONSTRAINED CASE

1303 The gradients for the simplex-constrained objective function are, $l < L_d$,
 1304

$$\begin{aligned} 1305 \frac{\partial O}{\partial a_{dl}} &= \beta_{dl} A_{dl} + \sum_{l^{(a)} \neq l} \beta_{dl^{(a)}} \left(\frac{-\exp(a_{dl}) \exp(a_{dl^{(a)}})}{\{1 + \sum_{l^{(m)}=1}^{L_d-1} \exp(a_{dl^{(m)}})\}^2} \right) \\ 1306 &+ \sum_{d, d' \neq d} \sum_{l'=1}^{L_{d'}-1} \gamma_{dl, d'l'} A_{dl} \frac{\exp(a_{d'l'})}{\{1 + \sum_{l'^{(m)}=1}^{L_{d'}-1} \exp(a_{d'l'^{(m)}})\}} \\ 1307 &+ \sum_{d, d' \neq d} \sum_{l^{(a)} \neq l} \sum_{l'=1}^{L_{d'}-1} \gamma_{dl^{(a)}, d'l'} \frac{-\exp(a_{dl}) \exp(a_{dl^{(a)}})}{\{1 + \sum_{l^{(m)}=1}^{L_d-1} \exp(a_{dl^{(m)}})\}^2} \frac{\exp(a_{d'l'})}{\{1 + \sum_{l'^{(m)}=1}^{L_{d'}-1} \exp(a_{d'l'^{(m)}})\}} \\ 1308 &- 2\lambda A_{dl} \left(\frac{\exp(a_{dl})}{\{1 + \sum_{l^{(m)}=1}^{L_d-1} \exp(a_{dl^{(m)}})\}} - p_{dl} \right) \\ 1309 &- 2\lambda \sum_{l^{(a)} \neq l} \left\{ \frac{-\exp(a_{dl}) \exp(a_{dl^{(a)}})}{\{1 + \sum_{l^{(m)}=1}^{L_d-1} \exp(a_{dl^{(m)}})\}^2} \left(\frac{\exp(a_{dl^{(a)}})}{\{1 + \sum_{l^{(m)}=1}^{L_d-1} \exp(a_{dl^{(m)}})\}} - p_{dl^{(a)}} \right) \right\} \\ 1310 &- 2\lambda \frac{\exp(a_{dl})}{\{1 + \sum_{l^{(m)}=1}^{L_d-1} \exp(a_{dl^{(m)}})\}^2} \sum_{l'=1}^{L_d-1} \left(\frac{\exp(a_{d'l'})}{\{1 + \sum_{l'^{(m)}=1}^{L_{d'}-1} \exp(a_{d'l'^{(m)}})\}} - p_{d'l'} \right), \end{aligned}$$

1311 where
 1312

$$A_{dl} = \frac{\exp(a_{dl}) \{1 + \sum_{l^{(m)}=1}^{L_d-1} \exp(a_{dl^{(m)}}) - \exp(a_{dl})\}}{\{1 + \sum_{l^{(m)}=1}^{L_d-1} \exp(a_{dl^{(m)}})\}^2}.$$

1313
 1314 A.I.5 GRADIENTS FOR OBTAINING THE VARIANCE-CONSTRAINED OPTIMAL
 1315 STOCHASTIC INTERVENTION IN THE TWO-WAY CONSTRAINED CASE UNDER A
 1316 FULLY PARAMETERIZED MODEL UNDER FORCED CHOICE

1317 The objective is
 1318

$$\begin{aligned} 1319 O(\boldsymbol{\pi}^a, \boldsymbol{\pi}^b) &= Q(\boldsymbol{\pi}^a, \boldsymbol{\pi}^b) - \lambda (\|\mathbf{p} - \boldsymbol{\pi}^a\|^2 + \|\mathbf{p} - \boldsymbol{\pi}^b\|^2) \\ 1320 &= \tilde{\mu} + \sum_{d=1}^D \sum_{l=1}^{L_d} \beta_{dl} (\pi_{dl}^* - \pi_{dl}^b) \\ 1321 &+ \sum_{d', d'': d' < d''} \sum_{l'=1}^{L_{d'}} \sum_{l''=1}^{L_{d''}} \gamma_{d'l', d''l''} (\pi_{d'l'}^* \pi_{d'l''}^* - \pi_{d'l'}^b \pi_{d'l''}^b) \\ 1322 &- \lambda \sum_{\# \in \{*, b\}} \sum_{d'''=1}^D \left\{ \sum_{l'''=1}^{L_d} (\pi_{d'''l'''}^{\#} - p_{d'''l'''}^{\#})^2 \right\} \end{aligned}$$

1323
 1324
 1325
 1326
 1327
 1328
 1329
 1330
 1331
 1332
 1333
 1334
 1335
 1336
 1337
 1338
 1339
 1340
 1341
 1342
 1343
 1344
 1345
 1346
 1347
 1348
 1349

1350 A.I.6 GRADIENTS FOR OBTAINING THE VARIANCE-CONSTRAINED OPTIMAL
 1351 STOCHASTIC INTERVENTION IN THE TWO-WAY CONSTRAINED CASE UNDER A
 1352 FULLY PARAMETERIZED MODEL

1353 With a fully parameterized, ANOVA-type model, we have:

1355
$$Q(\mathbf{a}) = \beta_0 + \sum_{d=1}^D \sum_{l=1}^{L_d} \beta_{dl} \cdot \frac{1}{1 + \exp(-a_{dl})} + \sum_{d',d''} \sum_{d' < d''} \sum_{l'=1}^{L_{d'}} \sum_{l''=1}^{L_{d''}} \gamma_{d'l',d''l''} \pi_{d'l'} \pi_{d''l''}.$$

1358 The gradients for the simplex-constrained objective function are, $l < L_d$,

$$\begin{aligned} \frac{\partial O}{\partial a_{dl}} &= \beta_{dl} A_{dl} + \sum_{l^{(a)} \neq l} \beta_{dl^{(a)}} \left(\frac{-\exp(a_{dl}) \exp(a_{dl^{(a)}})}{\{1 + \sum_{l^{(m)}=1}^{L_d-1} \exp(a_{dl^{(m)}})\}^2} \right) \\ &\quad + \sum_{d,d' \neq d} \sum_{l'=1}^{L_{d'}} \gamma_{dl,d'l'} A_{dl} \frac{\exp(a_{d'l'})}{\{1 + \sum_{l'^{(m)}=1}^{L_{d'}-1} \exp(a_{d'l'^{(m)}})\}} \\ &\quad + \sum_{d,d' \neq d} \sum_{l^{(a)} \neq l} \sum_{l'=1}^{L_{d'}} \gamma_{dl^{(a)},d'l'} \frac{-\exp(a_{dl}) \exp(a_{dl^{(a)}})}{\{1 + \sum_{l^{(m)}=1}^{L_d-1} \exp(a_{dl^{(m)}})\}^2} \frac{\exp(a_{d'l'})}{\{1 + \sum_{l'^{(m)}=1}^{L_{d'}-1} \exp(a_{d'l'^{(m)}})\}} \\ &\quad - 2\lambda A_{dl} \left(\frac{\exp(a_{dl})}{\{1 + \sum_{l^{(m)}=1}^{L_d-1} \exp(a_{dl^{(m)}})\}} - p_{dl} \right) \\ &\quad - 2\lambda \sum_{l^{(a)} \neq l} \left\{ \frac{-\exp(a_{dl}) \exp(a_{dl^{(a)}})}{\{1 + \sum_{l^{(m)}=1}^{L_d-1} \exp(a_{dl^{(m)}})\}^2} \left(\frac{\exp(a_{dl^{(a)}})}{\{1 + \sum_{l^{(m)}=1}^{L_d-1} \exp(a_{dl^{(m)}})\}} - p_{dl^{(a)}} \right) \right\} \\ &\quad - 2\lambda \frac{\exp(a_{dl})}{\{1 + \sum_{l^{(m)}=1}^{L_d-1} \exp(a_{dl^{(m)}})\}^2} \sum_{l'=1}^{L_d-1} \left(\frac{\exp(a_{dl'})}{\{1 + \sum_{l'^{(m)}=1}^{L_{d'}-1} \exp(a_{dl'^{(m)}})\}} - p_{dl'} \right), \end{aligned}$$

1378 where

$$A_{dl} = \frac{\exp(a_{dl}) \{1 + \sum_{l^{(m)}=1}^{L_d-1} \exp(a_{dl^{(m)}}) - \exp(a_{dl})\}}{\{1 + \sum_{l^{(m)}=1}^{L_d-1} \exp(a_{dl^{(m)}})\}^2}.$$

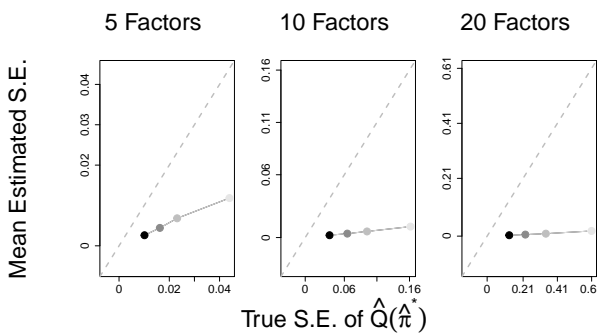
1383 A.I.7 OBJECTIVE FUNCTION IN UNCONSTRAINED SPACE

$$\begin{aligned} O(\mathbf{a}) &= Q(\mathbf{a}) - \lambda_n \|\mathbf{p} - \boldsymbol{\pi}\|^2 \\ &= \beta_0 + \sum_{d=1}^D \sum_{l=1}^{L_d-1} \beta_{dl} \frac{\exp(a_{dl})}{\{1 + \sum_{l^{(m)}=1}^{L_d-1} \exp(a_{dl^{(m)}})\}} \\ &\quad + \sum_{d',d''} \sum_{d' < d''} \sum_{l'=1}^{L_{d'}-1} \sum_{l''=1}^{L_{d''}-1} \gamma_{d'l',d''l''} \frac{\exp(a_{d'l'})}{\{1 + \sum_{l'^{(m)}=1}^{L_{d'}-1} \exp(a_{d'l'^{(m)}})\}} \frac{\exp(a_{d''l''})}{\{1 + \sum_{l''^{(m)}=1}^{L_{d''}-1} \exp(a_{d''l''^{(m)}})\}} \\ &\quad - \lambda_n \sum_{d'''=1}^D \left\{ \sum_{l'''=1}^{L_{d'''}-1} \left(\frac{\exp(a_{d'''l'''})}{\{1 + \sum_{l'''^{(m)}=1}^{L_{d'''}-1} \exp(a_{d'''l'''^{(m)}})\}} - p_{d'''l'''}) \right)^2 \right. \\ &\quad \left. + \left(1 - \left[\sum_{l'''=1}^{L_{d'''}-1} \frac{\exp(a_{d'''l'''})}{\{1 + \sum_{l'''^{(m)}=1}^{L_{d'''}-1} \exp(a_{d'''l'''^{(m)}})\}} \right] - \left(1 - \left[\sum_{l'''=1}^{L_{d'''}-1} p_{d'''l'''}) \right] \right) \right)^2 \right\} \end{aligned}$$

1399 APPENDIX II: SUPPLEMENTARY SIMULATION RESULTS

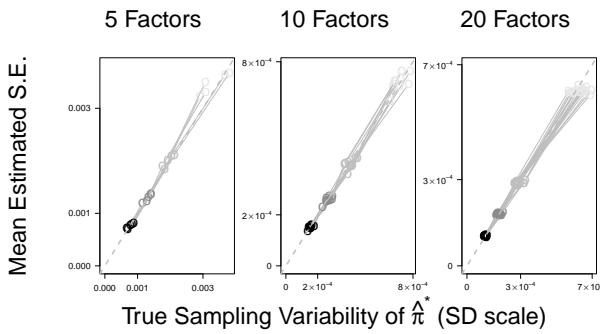
1400 A.I.8 SUPPLEMENTARY SIMULATION RESULTS WITH THE TWO-STEP ESTIMATOR

1401 A.I.9 ESTIMATION DETAILS



1422
1423
1424

Figure A.I.1: Points depict the average estimated standard deviation obtained via the Delta
method. Colors depict the sample size (with $n = 500$ being light gray and $n=10,000$ being
black).



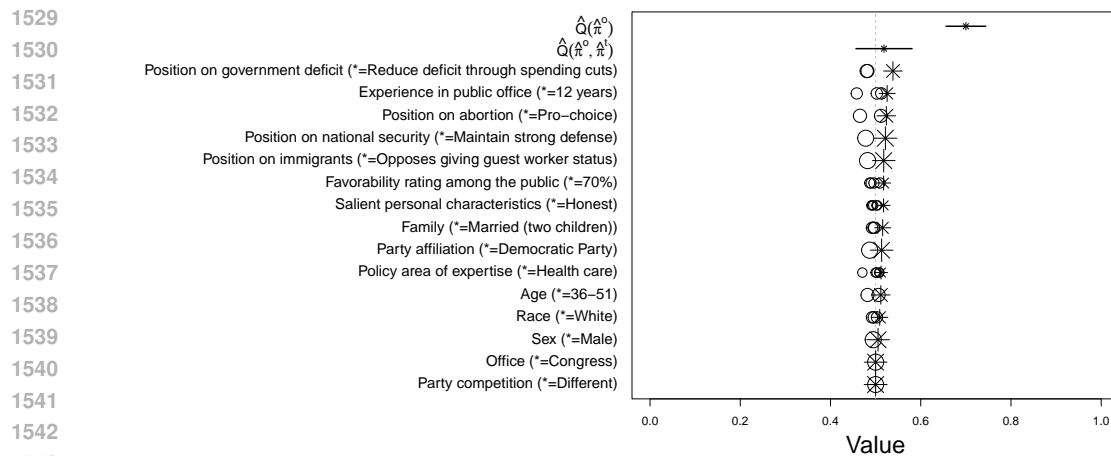
1450
1451
1452

Figure A.I.2: True sampling variability of $\hat{\pi}^*$ plotted against the variability estimated via
asymptotic inference. Colors depict the sample size (with $n=500$ being light gray and
 $n=10,000$ being black).

1453
1454
1455
1456
1457

1458 APPENDIX III: ADDITIONAL APPLICATION RESULTS
14591460 A.III.1 MAPPING THE 2016 CANDIDATE PRIMARY FEATURES ONTO THE CONJOINT
1461 LEVELS OF ONO & BURDEN (2019)
14621463 We map the features of the 2016 presidential election candidates onto the conjoint features of
1464 Ono & Burden (2019). In some cases, this mapping is straightforward (e.g., with candidate
1465 gender). In other cases, the mapping is less straightforward. For example, the factor levels
1466 associated with marital status do not encompass the full range of possibilities seen among
1467 2016 candidates. In such cases, we select the closest mapping (see Replication Data for full
1468 details). For example, a real, married candidate with 4 children would be mapped to the
1469 “Married with 2 children” level (not the “Single, divorced” or “Married, no children” levels).
14701471 We will explore these substantive questions by integrating the experiment mentioned above
1472 from Ono & Burden (2019). In this election, 17 Republican and 6 Democrat candidates
1473 vied for their respective partie’ nomination in primaries. These candidates have a large
1474 number of features, which we mapped onto the conjoint factors of Ono & Burden (2019)
(see §A.III.1 for details). Below we present this mapping for four of the candidates:
14751476 * *Ben Carson*: Republican, Black, male, 68-76, married (with children), 0 years of
1477 political experience, compassionate, policy focus on health care, emphasis on main-
1478 taining strong defense, opposes giving guest worker status, pro-life, don’t reduce
1479 deficit now.
1480 * *Hillary Clinton*: Democrat, White, female, 68-76, married (with children), 16 years
1481 of political experience, provides strong leadership, foreign policy, maintains strong
1482 defense, favors giving guest worker status, pro-choice, don’t reduce deficit now.
1483 * *Bernie Sanders*: Democrat, White, male, 68-76, married (with children), 34 years of
1484 political experience, compassionate, policy focus on economy, cut military budget,
1485 ambiguous position on immigration, pro-choice, reduce deficit through tax increase.
1486 * *Donald Trump*: Republican, White, male, 68-76, married (with children), 0 years of
1487 political experience, provides strong leadership, policy focus on economy, emphasis
1488 on maintaining strong defense, opposes giving guest worker status, pro-life, reduce
1489 deficit through spending cuts.
14901491 *Implementation Details*: Implementation deploys JAX for performing differentiable opti-
1492 mization routines. All analyses run in under 12 hours on consumer-grade PC hardware
1493 (CPU or GPU).
1494
1495
1496
1497
1498
1499
1500
1501
1502
1503
1504
1505
1506
1507
1508
1509
1510
1511

1512
 1513
 1514
 1515
 1516
 1517
 1518
 1519
 1520
 1521
 1522
 1523
 1524
 1525
 1526
 1527
 1528



1544 Figure A.III.1: Expected optimized vote share in the population in the average (uniform)
 1545 case (denoted by $\hat{Q}(\hat{\pi}^a)$), compared against factor-wise marginal means. The * for the
 1546 marginal means indicates the level with the highest marginal outcome (with that level listed
 1547 on the right-hand side of the figure along with the factor name). $\hat{Q}(\hat{\pi}^a, \hat{\pi}^b)$ denotes the
 1548 expected optimized vote share in the population under adversarial conditions compared
 1549 against factor-wise marginal means.

1550
 1551
 1552
 1553
 1554
 1555
 1556
 1557
 1558
 1559
 1560
 1561
 1562
 1563
 1564
 1565

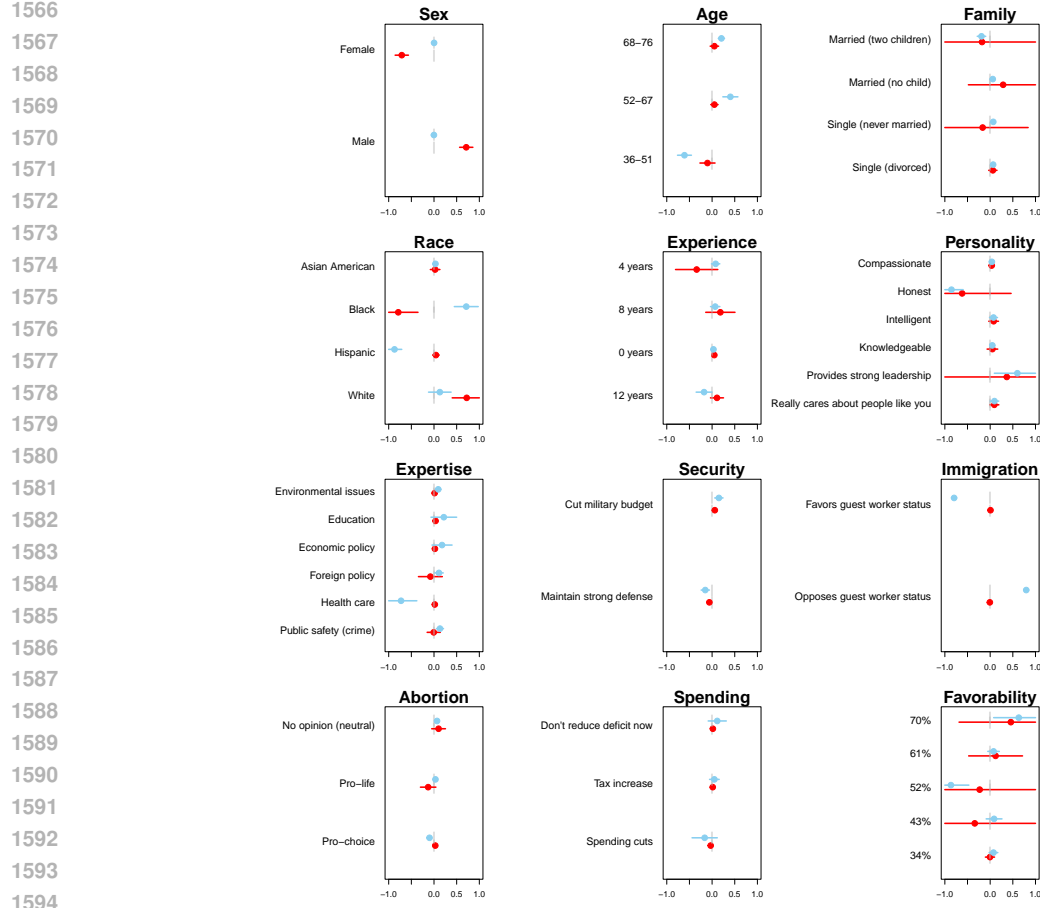


Figure A.III.2: Comparing optimal strategies in the non-adversarial vs. adversarial setting. Blue and red denote the equilibrium strategy for the agent facing Democratic and Republican voters in the primary stage, respectively.

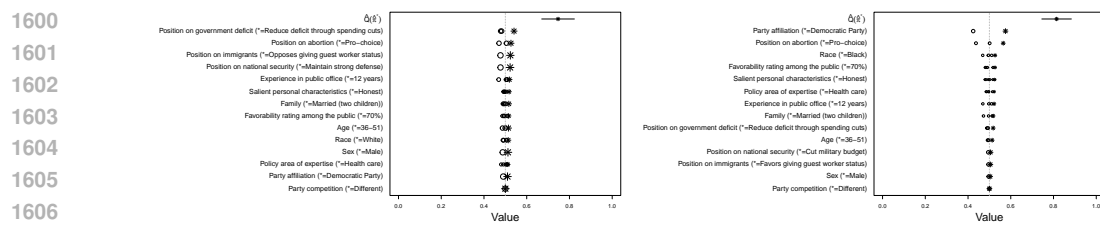


Figure A.III.3: Marginal means analysis, among all (left) and Democrat respondents (right).

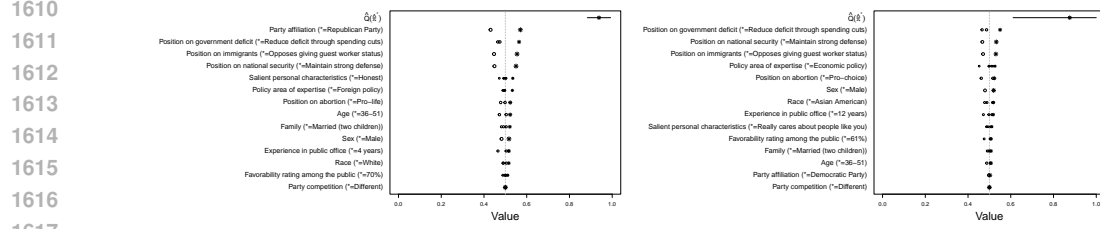


Figure A.III.4: Marginal means analysis, among Republican (left) and Independent (right) respondents.

1620
 1621
 1622
 1623
 1624
 1625
 1626
 1627
 1628
 1629
 1630
 1631
 1632
 1633
 1634
 1635
 1636
 1637
 1638
 1639
 1640
 1641
 1642
 1643
 1644
 1645
 1646
 1647
 1648
 1649
 1650
 1651
 1652
 1653
 1654
 1655
 1656
 1657
 1658
 1659
 1660
 1661
 1662
 1663
 1664
 1665
 1666
 1667
 1668
 1669
 1670
 1671
 1672
 1673

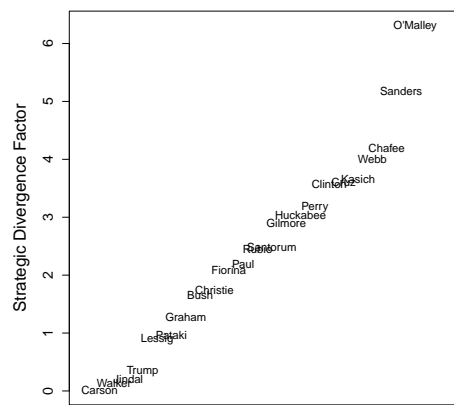


Figure A.III.5: Strategic divergence factor computed for major candidates in the 2016 primaries.